Quantifying the Summertime Response of the Austral Jet Stream and Hadley Cell to Stratospheric Ozone and Greenhouse Gases

EDWIN P. GERBER

Center for Atmosphere Ocean Science, Courant Institute of Mathematical Sciences, New York University, New York, New York

SEOK-WOO SON

School of Earth and Environmental Sciences, Seoul National University, Seoul, South Korea

(Manuscript received 2 September 2013, in final form 21 March 2014)

ABSTRACT

The impact of anthropogenic forcing on the summertime austral circulation is assessed across three climate model datasets: the Chemistry–Climate Model Validation activity 2 and phases 3 and 5 of the Coupled Model Intercomparison Project. Changes in stratospheric ozone and greenhouse gases impact the Southern Hemisphere in this season, and a simple framework based on temperature trends in the lower polar stratosphere and upper tropical troposphere is developed to separate their effects. It suggests that shifts in the jet stream and Hadley cell are driven by changes in the upper-troposphere–lower-stratosphere temperature gradient. The mean response is comparable in the three datasets; ozone has chiefly caused the poleward shift observed in recent decades, while ozone and greenhouse gases largely offset each other in the future.

The multimodel mean perspective, however, masks considerable spread in individual models' circulation projections. Spread resulting from differences in temperature trends is separated from differences in the circulation response to a given temperature change; both contribute equally to uncertainty in future circulation trends. Spread in temperature trends is most associated with differences in polar stratospheric temperatures, and could be narrowed by reducing uncertainty in future ozone changes. Differences in tropical temperatures are also important, and arise from both uncertainty in future emissions and differences in models' climate sensitivity. Differences in climate sensitivity, however, only matter significantly in a high emissions future. Even if temperature trends were known, however, differences in the dynamical response to temperature changes must be addressed to substantially narrow spread in circulation projections.

1. Introduction

Significant trends in the atmospheric circulation have been observed in the Southern Hemisphere during austral summer in recent decades (e.g., Thompson et al. 2011). The extratropical jet, or jet stream, has shifted poleward (Marshall 2003), accompanied by an expansion of the Hadley cell (Seidel and Randel 2007) and a redistribution of precipitation associated with the shift in the subtropical dry zone and storm track (Kang et al. 2011). Measurements of passive tracers in the Southern Ocean suggest increased ventilation of deep water, the expected oceanic response to an increased wind stress over the Southern Ocean associated with the jet shift (Waugh et al. 2013).

The poleward shift of jet stream and Hadley cell in austral summer have been attributed chiefly to the impact of stratospheric ozone loss (e.g., Polvani et al. 2011). The Antarctic ozone hole forms each spring, with peak depletion observed in October (Farman et al. 1985). The loss of ozone leads to anomalous cooling, appearing first in the upper stratosphere where radiative time scales are comparatively faster and descending to the tropopause by November and December. Thompson and Solomon (2002) show that this cooling and the associated fall in geopotential height in the stratosphere leads to a drop in tropospheric height over the pole in December: a poleward shift in the jet stream. A modeling study by Gillett and Thompson (2003) confirmed that the tropospheric response was associated with stratospheric cooling.

Corresponding author address: Edwin P. Gerber, Courant Institute of Mathematical Sciences, 251 Mercer Street, New York, NY 10012.
E-mail: gerber@cims.nyu.edu

DOI: 10.1175/JCLI-D-13-00539.1

© 2014 American Meteorological Society

It is also known that increasing greenhouse gases tend to shift the circulation poleward (e.g., Yin 2005; Butler et al. 2010). While greenhouse gases exhibit little seasonal cycle, Kushner et al. (2001) found that the largest response of the jet in a double CO_2 experiment was observed in austral summer. A growing body of evidence, however, indicates that the response of the jet stream in recent decades has been dominated by ozone. Chemistry–climate models with prognostic stratospheric chemistry to predict ozone changes (Perlwitz et al. 2008; McLandress et al. 2011), atmospheric models with prescribed ozone (Arblaster and Meehl 2006; Polvani et al. 2011), and multimodel datasets (Son et al. 2008, 2010) consistently show that ozone loss has dominated the summertime response. Based on nonlinear analysis with self-organizing maps (SOMs), Lee and Feldstein (2013) find further evidence for the dominance of ozone based on the reanalysis record.

In this study, we construct a simple framework to relate changes in the Southern Hemisphere circulation to changes in temperature in the polar stratosphere and tropical upper troposphere driven by ozone and greenhouse gases, respectively. The simple model builds on the findings of Arblaster et al. (2011) and Wilcox et al. (2012) that trends in the austral jet stream in coupled climate models are closely linked to changes in the temperature gradients in the upper troposphere and lower stratosphere. Our framework allows us to partition the response of the jet stream and Hadley cell to ozone and greenhouse gases in each individual model from phases 3 and 5 of the Coupled Model Intercomparison Project (CMIP3 and CMIP5) and Chemistry–Climate Model Validation activity 2 (CCMVal2) datasets.

We find that multimodel mean response is fairly uniform across all three datasets. Consistent with previous studies, ozone loss has dominated the response in the twentieth century, and both forcings tend to cancel each other out in the twenty-first century, although greenhouse gases begin to dominate in high emission scenarios. The multimodel mean trends, however, hide a significant degree of spread in model projections. The simple framework allows us to separate differences in the circulation trends resulting from 1) differences in the temperature trends and 2) differences in the models' dynamical response to temperature changes. For the CMIP5 models, we can also estimate the impact of natural variability.

The first source of uncertainty includes uncertainties in future emissions and ozone recovery and differences in climate sensitivity: how much will the world warm in response to greenhouse gas changes, or, in the case of ozone, how much will the stratosphere cool or warm in response to ozone loss or recovery? Overall, we find that differences in ozone related temperature trends in the lower polar stratosphere play a larger role in the intermodel spread in circulation trends than differences in warming trends in the tropical troposphere related to greenhouse gas changes. Reducing uncertainty in climate sensitivity will help reduce the spread in circulation trends, particularly if we follow a high greenhouse gas emissions scenario, but efforts to better constrain the recovery of ozone could potentially have a larger impact on reducing the spread in projections.

A second source of model spread is distinct from the upper-troposphere–lower-stratosphere temperature trends; even if we knew the gross thermodynamic response of the atmosphere to anthropogenic forcing, models would not agree on the circulation response. To differentiate this source of uncertainty from the impact of climate sensitivity, we term this source of model spread a "circulation sensitivity." Our framework suggests that these differences in the large-scale circulation response contribute equally to intermodel spread as differences in the thermal forcing.

We detail the datasets and develop our simple attribution framework in sections 2 and 3. The framework can be equally applied to the jet stream or the Hadley cell, and we focus on the jet stream, presenting the results in section 4. Section 5 then explores the origin behind the spread in model projections in greater detail. We discuss the relationship between jet stream trends and the expansion of the Hadley cell in section 6 and summarize and discuss the implications our study in section 7.

2. Datasets

Output was obtained from 55 models that participated in three multimodel intercomparison projects, as listed in Tables 1–3. The CMIP3 (Meehl et al. 2007) and CMIP5 (Taylor et al. 2012) models are coupled atmosphere–ocean climate models. Except for three models in the CMIP5, these models do not simulate stratospheric ozone chemistry, and hence stratospheric ozone was prescribed. The concentrations of carbon dioxide and other greenhouse gases are also specified. The twentieth-century CMIP3 and CMIP5 integrations were forced with the twentieth-century climate simulation (20C3M) and historical scenarios, respectively, which are based on past observations. For the future, we consider A1B scenario integrations from the CMIP3 models (a "middle of the road" future with only modest efforts to curtain greenhouse gases) and the representative concentration pathway 4.5 and 8.5 (RCP4.5 and RCP8.5) scenarios integrations from the CMIP5, where the total greenhouse gas radiative forcing reaches 4.5 and 8.5 W m^{-2} by the end of the century. These pathways fall on both sides of the A1B scenario, characterizing a future with more substantial efforts to

TABLE 1. The CMIP3 integrations assessed in this study. Models with fixed and time-varying ozone were partitioned as in Son et al. (2010), and models that prescribed time-varying ozone only in the historical period were omitted. Single integrations were obtained from the models with fixed ozone, but all ensemble members available in the data archive were analyzed for the models with time-varying ozone, with the number indicated in columns 4 and 5.

No.	Model acronym	Expanded model name	20C3M (1960–99)	A1B (2000–79)
		Fixed O_3		
—	BCCR-BCM2.0	Bjerknes Centre for Climate Research Bergen Climate Model, version 2.0	1	1
—	CGCM3.1(T63)	Canadian Centre for Climate Modelling and Analysis (CCCma) Coupled Global Climate Model, version 3.1 (spectral T63 resolution)	1	1
—	CNRM-CM3	Centre National de Recherches Météorologiques Coupled Global Climate Model, version 3	1	1
—	GISS-AOM	Goddard Institute for Space Studies, Atmosphere–Ocean Model	1	1
—	FGOALS-g1.0	Flexible Global Ocean–Atmosphere–Land System Model gridpoint, version 1.0	1	1
—	INM-CM3.0	Institute of Numerical Mathematics Coupled Model, version 3.0	1	1
—	IPSL-CM4	L'Institut Pierre-Simon Laplace Coupled Model, version 4	1	1
—	MRI-CGCM2.3.2	Meteorological Research Institute Coupled Atmosphere–Ocean General Circulation Model, version 2.3.2	1	1
		Varying O_3		
1	CSIRO Mk3.0	Commonwealth Scientific and Industrial Research Organisation Mark 3.0	2	1
2	GFDL CM2.0	Geophysical Fluid Dynamics Laboratory Climate Model, version 2.0	3	1
3	GFDL CM2.1	Geophysical Fluid Dynamics Laboratory Climate Model, version 2.1	3	1
4	INGV-SXG	Instituto Nazionale di Geofisica e Vulcanologia, Scale Interaction Experiment–G model (SINTEX-G)	1	1
5	MIROC-3.2(medres)	Model for Interdisciplinary Research on Climate, version 3.2 (medium resolution)	3	3
6	ECHAM5/MPI-OM	ECHAM5/Max Planck Institute Ocean Model	4	4
7	CCSM3.0	Community Climate System Model, version 3	8	7
8	PCM1	Parallel Climate Model, version 1	4	4
9	HadCM3	Hadley Centre Coupled Model, version 3	2	1
10	HadGEM1	Hadley Centre Global Environment Model, version 1	2	1

curtail emissions or little effort at all, and so allow us to characterize the impact of uncertainty in future emissions.

Models from the CCMVal2 (Eyring et al. 2010) simulate stratospheric chemistry, allowing them to predict stratospheric ozone concentrations based on specified mixing ratios of chlorofluorocarbons and other ozone depleting substances. In general they have better resolution and representation of stratospheric processes than the CMIP models, although roughly half of the CMIP5 models have sought to include a well-represented stratosphere (Charlton-Perez et al. 2013). With the exception of CMAM, however, the CCMVal2 models do not include a dynamic ocean. Observed sea surface temperatures (SSTs) are used to drive the historical simulations (REF-B1), while SSTs taken from a related coupled climate model simulation are used to drive the future scenario integrations (REF-B2). Carbon dioxide and other greenhouse gases are the same as those in the A1B scenario for the CMIP3 models, but it is important to stress that the specified SSTs highly constrain the warming response of these models.

As discussed by Son et al. (2010), not all CMIP3 models included time-varying ozone. Only the 10 models with time-varying ozone are used in this study (except for the calculations shown in Figs. 1 and A1). The ozone concentrations that they used, however, were not archived. Eyring et al. (2013) investigate the treatment of ozone in the CMIP5 models. As listed in Table 3, roughly half used a zonal mean stratospheric ozone dataset developed through a joint effort of the International Global Atmospheric Chemistry (IGAC) and Stratosphere–Troposphere Processes and their Role in Climate (SPARC) activities (Cionni et al. 2011) or a slight modification thereof to allow for a solar cycle in the future. The other modeling groups made different choices, some basing their ozone concentrations on a related chemistry–climate model, and three simulated interactive ozone chemistry.

3. A simple framework to assess the circulation response to anthropogenic forcing

It is well established that gradients in temperature and moisture between the tropics and polar regions drive the

TABLE 2. The CCMVal2 integrations assessed in this study. These models simulate interactive ozone chemistry but, with the exception of CMAM, are forced with prescribed sea surface temperatures. Columns 4 and 5 indicate the number of ensemble members that were analyzed.

No.	Model acronym	Expanded model name	REF-B1 (1960–99)	REF-B2 (2000–79)
11	CAM3.5	Community Atmosphere Model, version 3.5	1	1
12	CCSRNIES	Center for Climate-Systems Research–National Institute of Environmental Studies	1	1
13	CMAM	Canadian Middle Atmosphere Model	3	3
14	CNRM-ACM	Centre National de Recherches Météorologiques Atmospheric Climate Model	2	1
15	GEOSCCM	Goddard Earth Observing System Chemistry–Climate Model	1	1
16	MRI	Meteorological Research Institute	4	2
17	SOCOL	Solar–Climate–Ozone Links	3	3
18	UMSLIMCAT	Unified Model Single Layer Isentropic Model of Chemistry and Transport	1	1
19	UMUKCA-METO	Unified Model U.K. Chemistry and Aerosols Module–Met Office	1	1
20	WACCM	Whole Atmosphere Community Climate Model	4	3

large-scale atmospheric circulation (e.g., Lorenz 1967). Wilcox et al. (2012) found that austral jet trends in CMIP5 models are linked to changes in temperature gradients in the upper troposphere–lower stratosphere. Greenhouse gases and ozone can impact the large-scale circulation by altering these gradients. In particular, Butler et al. (2010) simulated changes in the large-scale circulation in response to greenhouse gas increases by warming the tropical upper troposphere in a simplified general circulation model (GCM). They found that the expansion of the Hadley cells and extratropical jets could be modeled with some quantitative accuracy, as compared with comprehensive models (see also Wang et al. 2012). Likewise, Polvani and Kushner (2002) captured the impact of ozone loss in a simple GCM by prescribing a cooling of the stratospheric polar vortex.

Figure 1 shows November–January (NDJ) temperature changes simulated by CMIP3 climate models over the periods 1960–99 and 2000–79. The season and intervals were chosen to highlight the impact of ozone loss and recovery. Ozone's influence is evident by comparing the top panels, based on eight models with fixed ozone, and the lower panels, based on 10 models with prescribed, time-varying ozone. In the late twentieth century, models with time-varying ozone exhibit cooling in excess of 10°C over the South Pole at 100 hPa (Fig. 1c). While increased greenhouse gases cool the stratosphere at upper levels, we can attribute the cooling at 100 hPa to ozone by comparing this against the models with fixed ozone (Fig. 1a), where there is little trend at this elevation. Temperatures over the polar cap nearly recover over the next eight decades in the models with time-varying ozone (Fig. 1d), in contrast to weak cooling trends in models with fixed ozone (Fig. 1b). This suggest that greenhouse gases have a minimal impact on this region of the stratosphere, allowing us to quantify the ozone impact by the polar cap average (64°–90°S) temperature change at 100 hPa (white boxes in Figs. 1c,d), which we denote ΔT_{polar}.

The impact of greenhouse gases on temperature gradients in the upper troposphere is also evident in Fig. 1, with peak warming in the tropics just below the tropopause near 200 hPa. Their influence is more evident in the twenty-first-century interval: this is due to both the exponential increase of CO_2 in the A1B scenario and the fact that this period is twice as long as the twentieth-century period. We use a longer period because it takes longer for ozone to recover than it did to destroy it, despite the success of the Montreal protocol in stopping chlorofluorocarbon emissions (e.g., Eyring et al. 2010). We quantify the impact of greenhouse gas forcing on the temperature changes at 200 hPa, averaged from 30°S to 30°N (black boxes in Figs. 1c,d), which we denote ΔT_{trop}. Arblaster et al. (2011) show that upper-tropospheric temperature trends are highly correlated with overall surface warming, so that variations in ΔT_{trop} in models forced by the same emissions reflect differences in the climate sensitivity.

Our idea is to relate the jet stream (or, equivalently, the Hadley cell) response to changes in temperature driven by ozone and greenhouse gases. Focusing on the jet stream, we quantify changes by the latitudinal shift in the 850-hPa zonal wind maximum ΔU_{lat} during December–February (DJF). A shift in the jet stream projects strongly onto the southern annular mode (SAM), and changes could equivalently be quantified as a shift in the SAM index, as in other studies (e.g., Arblaster and Meehl 2006). We then assume a linear relationship between changes in temperature and the jet,

TABLE 3. The CMIP5 integrations assessed in this study. Columns 4–6 indicate how many ensemble members were analyzed for each scenario. The final column indicates how the ozone was treated, as described in Eyring et al. (2013), using the Cionni et al. (2011) dataset (C), a different prescribed dataset (O), or that the model simulated interactive stratospheric ozone chemistry (I).

No.	Model acronym	Expanded model name	Historical (1960–99)	RCP4.5 (2007–79)	RCP8.5 (2007–79)	Ozone forcing
21	ACCESS1.0	Australian Community Climate and Earth-System Simulator, version 1.0	1	1	1	C
22	ACCESS1.3	Australian Community Climate and Earth-System Simulator, version 1.3	1	1	1	C
23	BCC-CSM1.1	Beijing Climate Center, Climate System Model, version 1.1	3	1	1	C
24	CCSM4	Community Climate System Model, version 4	6	6	6	O
25	CNRM-CM5	Centre National de Recherches Météorologiques Coupled Global Climate Model, version 5	10	1	1	I
26	CSIRO Mk3.6.0	Commonwealth Scientific and Industrial Research Organisation Mark 3.6.0	10	5	5	C
27	CanESM2	Second Generation Canadian Earth System Model	5	5	5	C*
28	FGOALS-g2	Flexible Global Ocean–Atmosphere–Land System Model gridpoint, version 2	5	1	1	C
29	FIO-ESM	First Institute of Oceanography Earth System Model	3	3	3	C
30	GFDL CM3	Geophysical Fluid Dynamics Laboratory Climate Model, version 3	5	1	1	I
31	GFDL-ESM2G	Geophysical Fluid Dynamics Laboratory Earth System Model with Generalized Ocean Layer Dynamics (GOLD) component	1	1	1	C
32	GFDL-ESM2M	Geophysical Fluid Dynamics Laboratory Earth System Model with Modular Ocean Model, version 4 (MOM4) component	1	1	1	C
33	GISS-E2-H	Goddard Institute for Space Studies Model E2, coupled with the Hybrid Coordinate Ocean Model	5	5	3	O
34	GISS-E2-R	Goddard Institute for Space Studies Model E2, coupled with the Russell ocean model	5	5	5	O
35	HadGEM2-CC	Hadley Centre Global Environment Model, version 2–Carbon Cycle	3	1	1	C*
36	HadGEM2-ES	Hadley Centre Global Environment Model, version 2–Earth System	4	1	1	C*
37	INM-CM4	Institute of Numerical Mathematics Coupled Model, version 4	1	1	1	C
38	IPSL-CM5A-LR	L'Institut Pierre-Simon Laplace Coupled Model, version 5A, low resolution	5	4	4	O
39	IPSL-CM5A-MR	L'Institut Pierre-Simon Laplace Coupled Model, version 5A, mid resolution	1	1	1	O
40	IPSL-CM5B-LR	L'Institut Pierre-Simon Laplace Coupled Model, version 5B, low resolution	1	1	1	O
41	MIROC-ESM-CHEM	Model for Interdisciplinary Research on Climate, Earth System Model, Chemistry Coupled	1	1	1	I
42	MIROC-ESM	Model for Interdisciplinary Research on Climate, Earth System Model	3	1	1	O
43	MIROC5	Model for Interdisciplinary Research on Climate, version 5	4	1	1	O
44	MPI-ESM-LR	Max Planck Institute Earth System Model, low resolution	3	3	3	C*
45	MPI-ESM-MR	Max Planck Institute Earth System Model, medium resolution	3	3	1	C*
46	MRI-CGCM3	Meteorological Research Institute Coupled Atmosphere–Ocean General Circulation Model, version 3	3	1	1	C
47	NorESM1-M	Norwegian Earth System Model, version 1 (intermediate resolution)	3	1	1	O

* Cionni et al. (2011) dataset was slightly modified.

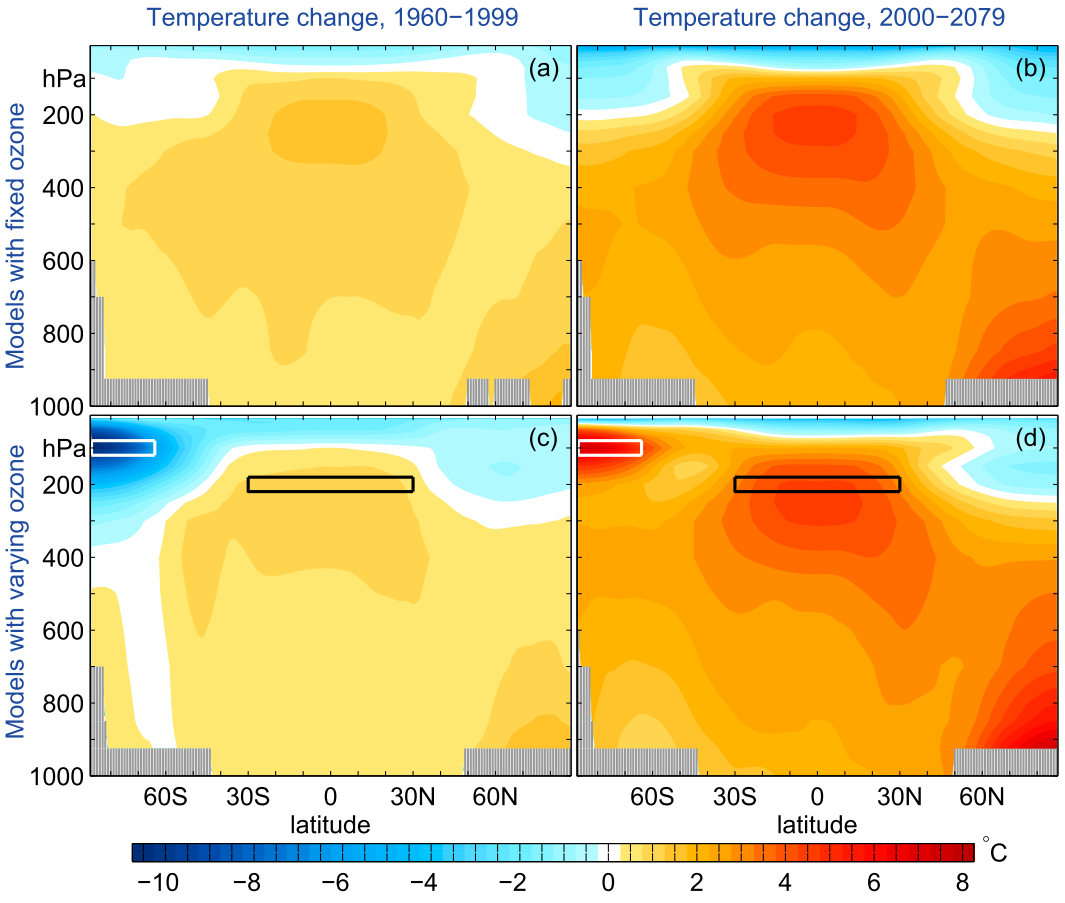

FIG. 1. Zonal mean temperature changes in NDJ during the periods of (a),(c) ozone loss (1960–99) and (b),(d) ozone recovery (2000–79) as simulated by CMIP3 models. Multimodel means are shown for (a),(b) models with fixed ozone and (c),(d) models that prescribed time-varying ozone. The total temperature change is computed by first calculating the linear trends over the 1960–99 and 2000–79 periods and then scaling the trends to represent the total change over 40 and 80 yr, respectively. The models in the fixed and time-varying ozone composites are identified in Table 1, and regions of missing data are masked in gray.

$$\Delta U_{\text{lat}} = r_{\text{polar}} \Delta T_{\text{polar}} + r_{\text{trop}} \Delta T_{\text{trop}}. \quad (1)$$

The goal is to determine the regression coefficients r_{polar} and r_{trop}, which quantify the sensitivity of the jet stream to changes in polar and tropical temperatures. They will in turn allow us to partition trends in the jet associated with changes in ozone and greenhouse gases.

To solve the linear system (1), trends over at least two periods are needed to determine the regression coefficients. Clearly, if short intervals were sampled, the results would be overwhelmed by interval variability. In addition, if the trends are not substantially different between the two periods, the system is ill conditioned and overly sensitive to noise in the data. We therefore focus on the two periods shown in Fig. 1 where the signals in ozone and greenhouse gases (GHG) are fairly orthogonal: 1960–99, where ozone is depleted and GHG are increasing, and 2000–79, where ozone is projected to recover and GHG continue to climb. For the CMIP5 models, we use the period 2007–79, to avoid interpolating between the historical and future scenarios.

We also optimized the seasonal timing of the temperature and jet shift signals. Thompson and Solomon (2002) found that the tropospheric response to stratospheric ozone changes lags changes in the stratosphere by about 1 month, and Son et al. (2010) found a similar lag in CCMVal2 models. To account for this lag and for slight differences in the formation of the ozone hole in different models, ΔT_{polar} is averaged over the months from October to January (ONDJ). The ΔT_{trop} and ΔU_{lat} are based on averages over the austral summer (DJF), as there is no known lag between tropical temperatures and the circulation. The results are essentially unchanged, however, if we alter the seasonal timing slightly: for example, measuring all temperatures in NDJ.

To minimize the impact of natural variability, we average the trends from all available ensemble integrations for each climate model. For each CCMVal2 and CMIP3 model, this gives us one mean trend in $\Delta U_{\rm lat}$, $\Delta T_{\rm polar}$, and $\Delta T_{\rm trop}$ for the late twentieth century and likewise for the twenty-first-century period of ozone recovery. From these six values we solve (1) exactly, obtaining $r_{\rm polar}$ and $r_{\rm trop}$ for each model. For the CMIP5 models, we collect ensemble mean trends from the three scenarios (historical, RCP4.5, and RCP8.5), making the system overdetermined. We therefore apply multiple linear regression to find the optimal coefficients.

The additional information for the CMIP5 models also allows us to test the robustness of the simple framework: how do the regression coefficients change if we remove one of the scenarios? We can solve (1) exactly if we keep just two of the CMIP5 scenarios. If we remove either the RCP4.5 or RCP8.5 integration, the values of $r_{\rm polar}$ are essentially unchanged. The multimodel mean value of $r_{\rm trop}$ is also very robust, and individual model values are unchanged if we remove the RCP4.5 data. The intermodel standard deviation in $r_{\rm trop}$ increases by about 50%, however, if we remove the RCP8.5 integrations. This suggests that the coefficients of $r_{\rm trop}$ are more constrained by the RCP8.5 integrations, where the global warming signal in the tropics is stronger. With the weaker warming in the RCP4.5, the decrease in the signal to noise ratio leads to more scatter in the estimate of $r_{\rm trop}$ but no systematic bias. If we instead remove the historical integrations, however, and try to fit the coefficients from the RCP4.5 and RCP8.5 integrations alone, the linear system becomes ill conditioned. The ozone signal is essentially the same in both cases, and the regression coefficients begin to vary wildly from model to model.

4. Partitioning the jet response to ozone and greenhouse gas forcing

The regression coefficients $r_{\rm polar}$ and $r_{\rm trop}$ for each of the models are shown in Fig. 2. With just two exceptions, $r_{\rm polar}$ is positive: cooling of the polar stratosphere is associated with a poleward shift in the jet stream. As detailed in section 4b, the model with a large negative coefficient, model 29 (FIO-ESM), may not have properly specified ozone trends. Removing this model, the average amplitude of $r_{\rm polar}$ is $0.20^\circ\,{\rm K}^{-1}$, with a standard error of $0.11^\circ\,{\rm K}^{-1}$: a 1-K cooling of the lower stratosphere over the polar cap is associated with roughly a $0.2^\circ \pm 0.1^\circ$ poleward shift of the jet. As shown more clearly in Fig. 3a, the amplitude of $r_{\rm polar}$ is overall larger in the CCMVal2 models. While this difference is not significant in terms of intermodel variability, the higher degree of sensitivity in the models with interactive ozone is consistent with the fact that models exhibit a larger tropospheric response to zonally asymmetric ozone anomalies, as compared to zonally symmetric anomalies of the same strength (e.g., Crook et al. 2008; Waugh et al. 2009).

With only a single exception, $r_{\rm trop}$ is negative: nearly all models associate tropical warming with a poleward shift in the jet stream. The average amplitude is $-0.32^\circ\,{\rm K}^{-1}$ with a standard error of $0.16^\circ\,{\rm K}^{-1}$: warming the tropics by 1 K shifts the jet roughly 0.3° poleward. That $r_{\rm trop} \approx -r_{\rm polar}$ indicates that the jet stream is comparably sensitive to cooling in the lower stratosphere or warming in the upper tropical troposphere: the temperature gradient in the upper troposphere–lower stratosphere appears to control the jet position.

a. The multimodel mean picture

Given the temperature trends, the regression coefficients allow us to partition the jet shift into portions associated with polar cooling ($r_{\rm polar}\Delta T_{\rm polar}$) and tropical warming ($r_{\rm trop}\Delta T_{\rm trop}$). Figure 3b shows the multimodel mean temperature trends over the period of ozone loss for each dataset. As we saw in Fig. 1, ozone-induced cooling of the polar stratosphere is nearly 2 K decade^{-1} over this period, nearly an order of magnitude stronger than the modest (albeit significant) warming of the tropical upper troposphere by about a ¼ K decade^{-1}. Since the regression coefficients indicate that the jet is about equally sensitive to polar cooling or tropical warming, the trends in the jet stream $\Delta U_{\rm lat}$, shown in Fig. 3c, are dominated by the ozone signal. The analysis suggests that the majority of the poleward jet shift, greater than 75% in the multimodel mean of each dataset, is associated with cooling of the polar stratosphere. This supports the conclusions of individual models where the ozone and greenhouse forcings were explicitly separated (e.g., Perlwitz et al. 2008; Polvani et al. 2011; McLandress et al. 2011).

A more recent study based on pattern analysis of zonal wind trends by Lee and Feldstein (2013) estimated that ozone contributed to three-fifths of the jet shift, less than our estimate. We were thus concerned that our method might overestimate the jet shift associated with ozone, particularly if greenhouse gas–induced cooling of the stratosphere aliases into $\Delta T_{\rm polar}$. We therefore explored polar stratospheric temperature changes in CMIP3 models with fixed ozone, as described in the appendix, and concluded that aliasing does not explain the difference. Briefly, we find that the polar stratosphere at 100 hPa tends to cool only a small amount in response to greenhouse gas increase, and this cooling

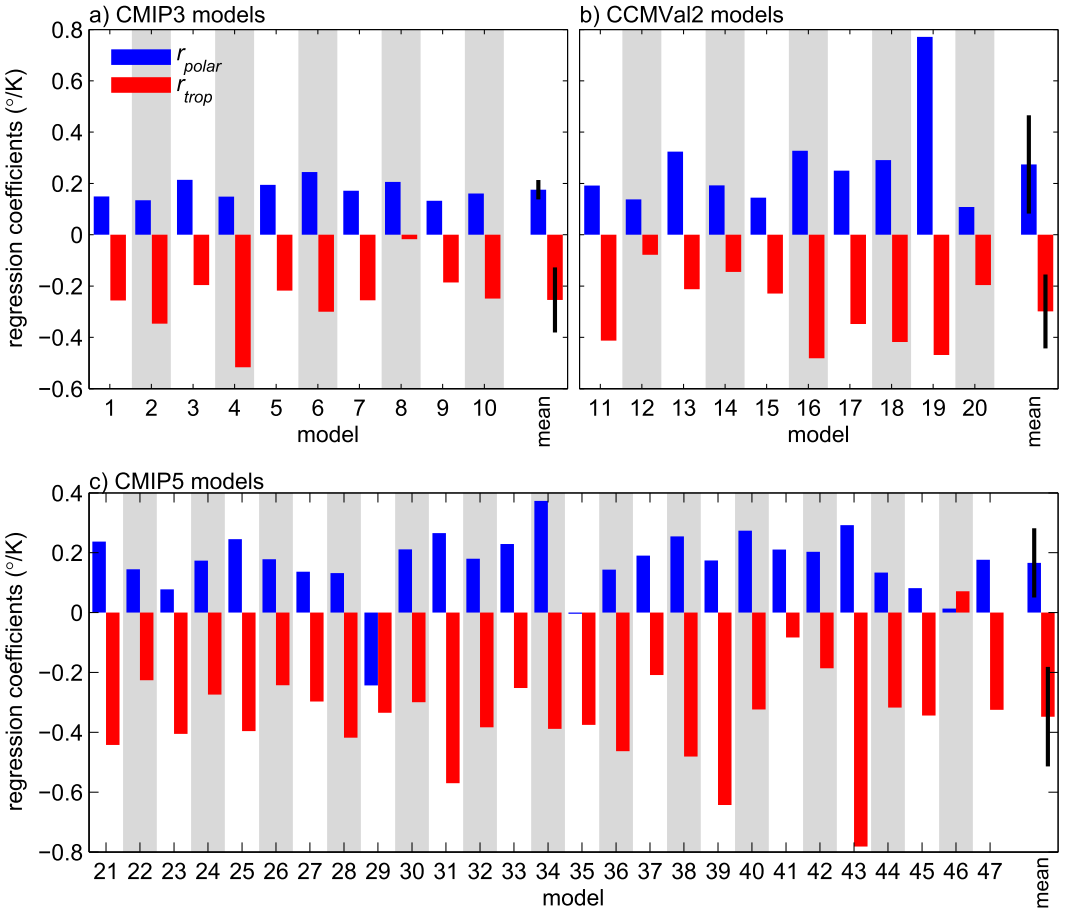

FIG. 2. The regression coefficients r_{polar} and r_{trop} computed for the (a) CMIP3, (b) CCMVal2, and (c) CMIP5 model simulations. The identity of each model is listed in Tables 1–3. Each coefficient expresses the shift (°lat) of the jet stream associated with a 1-K warming over the polar cap at 100 hPa or the tropics at 200 hPa. A positive regression coefficient suggests a northward (equatorward) shift of the jet stream associated with warming. The rightmost bars in each panel show the multimodel ensemble mean, with black lines indicating the ±1 standard deviation spread.

is not significantly correlated with the strength of the tropical warming. Moreover, models with enhanced tropical warming exhibit less polar cooling. Thus, an effort to account for links between ΔT_{trop} and ΔT_{polar} by regression would tend to amplify the ozone-induced response.

The CCMVal2 models in aggregate simulate a larger jet shift over the period of ozone loss, albeit not significantly given large intermodel spread. In comparison with the CMIP3 models, this difference can be attributed to enhanced sensitivity to stratospheric temperatures—larger values of r_{polar}—as the zonal mean cooling of the stratosphere is nearly identical. The jet response is further weakened in the CMIP5 models, but here it can be attributed to both weaker cooling of the polar stratosphere and smaller values of r_{polar}.

As established by Son et al. (2008, 2010) for the CMIP3, CCMVal1, and CCMVal2 models, the austral summer jet stream hardly moves during the period of ozone recovery (Fig. 3e). We find this to be the case in the CMIP5 RCP4.5 integrations models as well, but in the RCP8.5 integrations the jet shifts farther poleward, albeit more slowly than in the late twentieth century, as shown by Barnes et al. (2014).

The difference can be interpreted in terms of the temperature trends. Ozone recovery leads to a warming of the stratosphere (Fig. 3d), which by itself would tend to shift the jet stream equatorward. In this sense, the healing of the ozone hole seeks to undo the poleward shift driven during the period of ozone loss. Greenhouse gases, however, drive stronger warming in the future, pushing the jet poleward. In the CCMVal2, CMIP3, and CMIP5 RCP4.5 simulations, these effects cancel out and there is little net change. In the RCP4.5 integrations, there is less warming associated with ozone recovery but also less tropical warming, because of the weaker

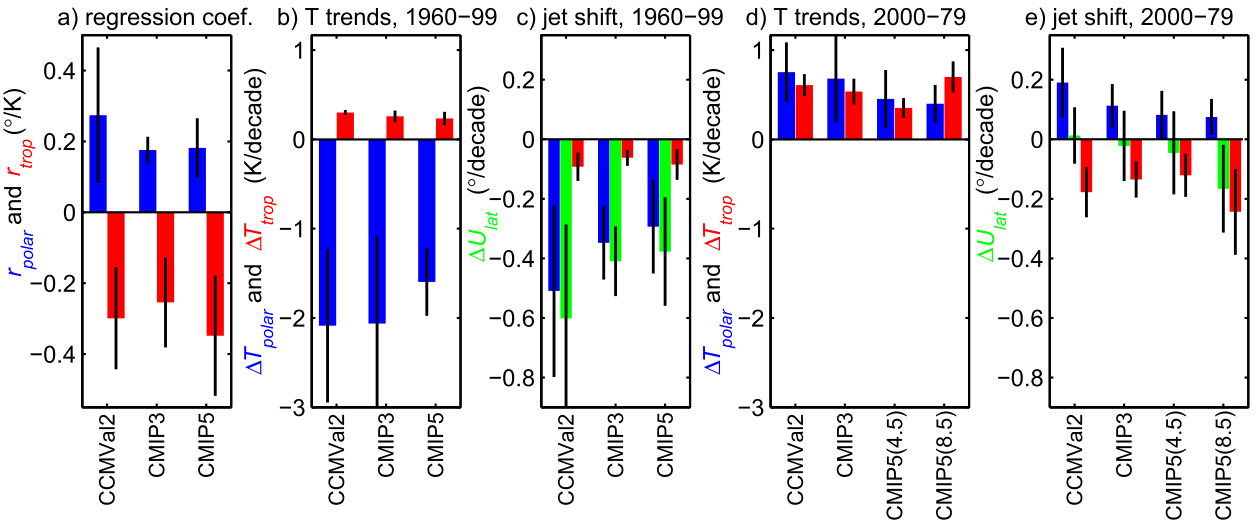

FIG. 3. A summary of the multimodel ensemble mean results for the CCMVal2, CMIP3, and CMIP5 datasets. (a) The mean values of the regression coefficients r_{polar} and r_{trop} in blue and red, respectively. Here and in following panels, black lines indicate the ±1 standard deviation spread. (b) The 1960–99 temperature trends ΔT_{polar} and ΔT_{trop} in blue and red. (c) The 1960–99 jet shift ΔU_{lat} in green, broken into the components associated with ozone ($r_{\text{polar}}\Delta T_{\text{polar}}$) and greenhouse gases ($r_{\text{trop}}\Delta T_{\text{trop}}$) in blue and red. (d),(e) As in (b),(c), but with focus on the period of anticipated ozone recovery: 2000–79 for the CCMVal2 and CMIP3 integrations, and 2007–79 for the CMIP5 RCP4.5 and RCP8.5 integrations. Model 29 has been removed before summarizing the CMIP5 results, as justified in section 4b.

greenhouse gas forcing in this scenario, and so the same impact on the equator-to-pole temperature gradient. In the CMIP5 RCP8.5 integrations, however, the stronger greenhouse gas forcing leads to significantly more warming in the tropics (nearly double that seen in the RCP4.5, consistent with the near doubling of the radiative forcing). This dominates the warming associated with ozone recovery: the equator-to-pole temperature gradient increases and the jet shifts poleward.

b. *Individual model results*

Results for each model separately are shown in Figs. 4–8. For the period of ozone loss, the jet shifts in the CMIP3 and CCMVal2 models are uniformly dominated by ozone-induced cooling of the polar stratosphere. More than two-thirds of the jet shift is associated with polar cooling in every single model, as seen in Figs. 4c,d. As with the multimodel mean, this is because the ozone cooling is substantially larger than tropical warming in every single model (Figs. 4a,b).

Trends from the twenty-first-century CMIP3 and CCMVal2 scenario integrations (Fig. 5) reveal a range of poleward and equatorward jet shifts. Accumulated over eight decades, these differences lead to a spread of approximately 3° in the jet shift. The CMIP3 trends in Figs. 5a,c suggest that differences in temperature trends can explain much of this spread. In models where ozone recovery drives a strong warming of the stratosphere in comparison to greenhouse gas–induced warming of the tropics (e.g., models 8 and 9), the jet shifts equatorward. In models where greenhouse gas–induced warming of the tropics dominates the warming of the stratosphere (e.g., models 2, 3, 5, 6, and 10), the jet shifts poleward. Note also that these differences are associated mostly with differences in stratospheric trends: while tropical warming varies by about a factor of 2 in the tropics, trends in the polar stratosphere vary by a factor of 10, from about 0.15 to 1.5 K decade^{-1}. This suggests that uncertainty in the thermal response to ozone recovery is a key source of model spread.

The situation is a bit muddier for the CMIP5 models. During the period of ozone loss (Fig. 6), polar cooling associated with ozone loss dominates the jet shift in 23 of the 27 models. In one other, model 45 (MPI-ESM-MR), ozone and greenhouse gases appear to have equal impact on the jet shift. Model 29 (FIO-ESM) is highly anomalous in that the stratosphere appears to warm during the period of ozone loss and then cool in the future (Figs. 7 and 8). The model behaves more like the CMIP3 model with fixed ozone, which suggests that ozone loss and recovery may not have been properly prescribed. We therefore omit this model from all further analyses in this study. In models 35 (HadGEM2-ES) and 46 (MRI-CGCM3), the jet shifts weakly poleward over the period of ozone loss and then more strongly poleward in the future (Figs. 7 and 8). Hence, the regression analysis indicates that polar stratospheric cooling

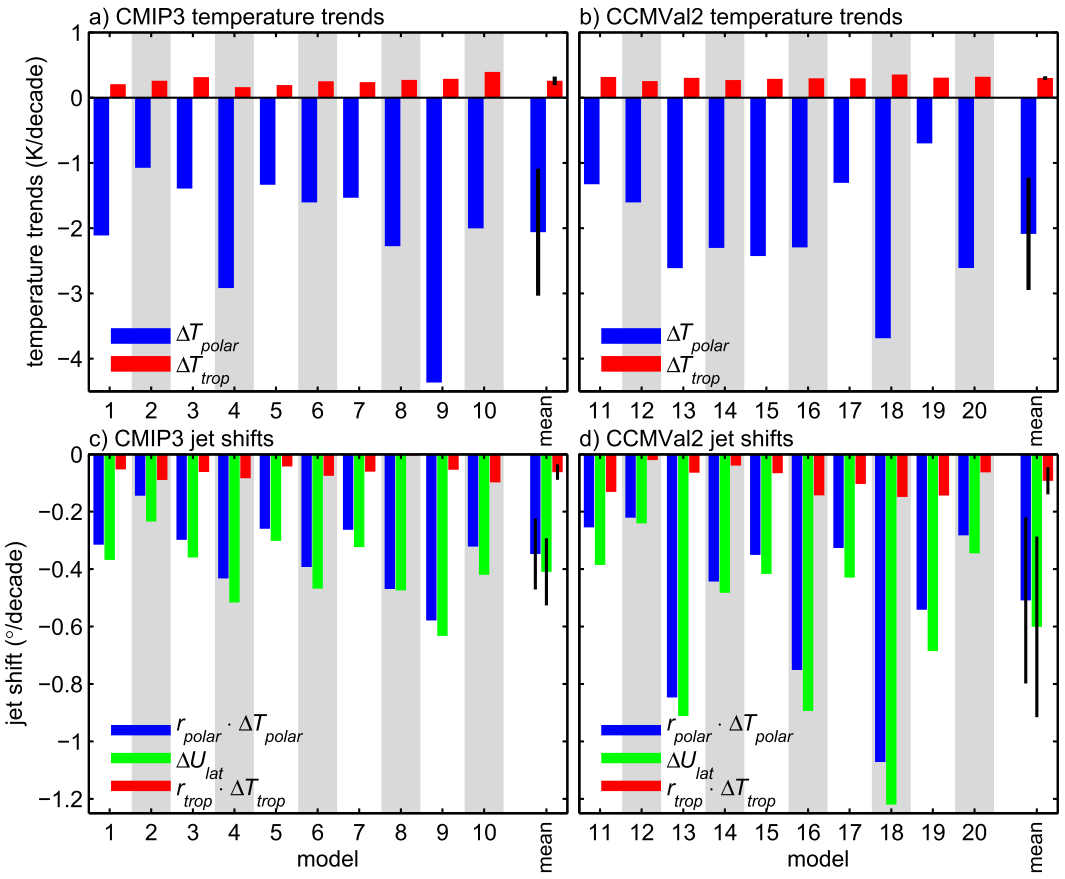

FIG. 4. (a),(b) Temperature and (c),(d) jet shift trends for CMIP3 and CCMVal2 during the period of ozone loss (1960–99). Here we expand the analysis shown for the multimodel means in Figs. 3b,c for the individual 20C3M and REF-B1 scenario integrations of the CMIP3 and CCMVal2 models, respectively.

or warming has almost no effect on jet position, as manifested by near-zero values of r_{polar} in Fig. 2.

Projections of future temperature and jet trends for the individual CMIP5 models are shown for the RCP4.5 and RCP8.5 scenarios in Figs. 7 and 8. The use of two scenarios allows us to assess uncertainty in the future emissions, and as a result the spread in future jet shifts increases relative to the CMIP3 or CCMVal2 models with a single emissions pathway. In the RCP4.5 projections, there is greater overall variance in jet trends associated with polar cooling: the standard deviation of $r_{\text{polar}}\Delta T_{\text{polar}}$ is 0.08° decade^{-1}, compared to 0.06° decade^{-1} for the jet shift associated with tropical warming, $r_{\text{trop}}\Delta T_{\text{trop}}$. In the RCP8.5 projections, the roles reverse. Polar cooling trends are associated with a comparable fraction of the variance, with a standard deviation of 0.08° decade^{-1}, but the variability associated with tropical warming doubles to 0.14° decade^{-1}. This motivates us to more carefully assess the sources of uncertainty, separating the influence of spread in the temperature trends from spread in the regression coefficients.

5. Quantifying sources of spread in jet projections

Two case studies of individual model integrations in Fig. 9 suggest multiple sources of spread in the CMIP5 model projections. The first comparison (Figs. 9a–c) highlights the impact of the polar stratosphere. We show projections from the two models with the most extreme equatorward and poleward jet shifts in the RCP4.5 dataset (Fig. 7b): GFDL CM3 (model 30) and IPSL-CM5A-MR (model 39). Figure 9a shows the jet position as a function of time for the two models, revealing a split of almost 5° over the period of 2007–79. The models do not even agree on the sign of the response: the jet shifts equatorward in the GFDL CM3 and poleward in IPSL-CM5A-MR.

Their global warming signal in the tropics, however, is nearly identical (Fig. 9b). Both models project a warming of approximately 4 K by 2080, suggesting that differences in climate sensitivity are not responsible for the divergence of the jet trends. The y axis is inverted to reflect the fact that the jet position in negatively

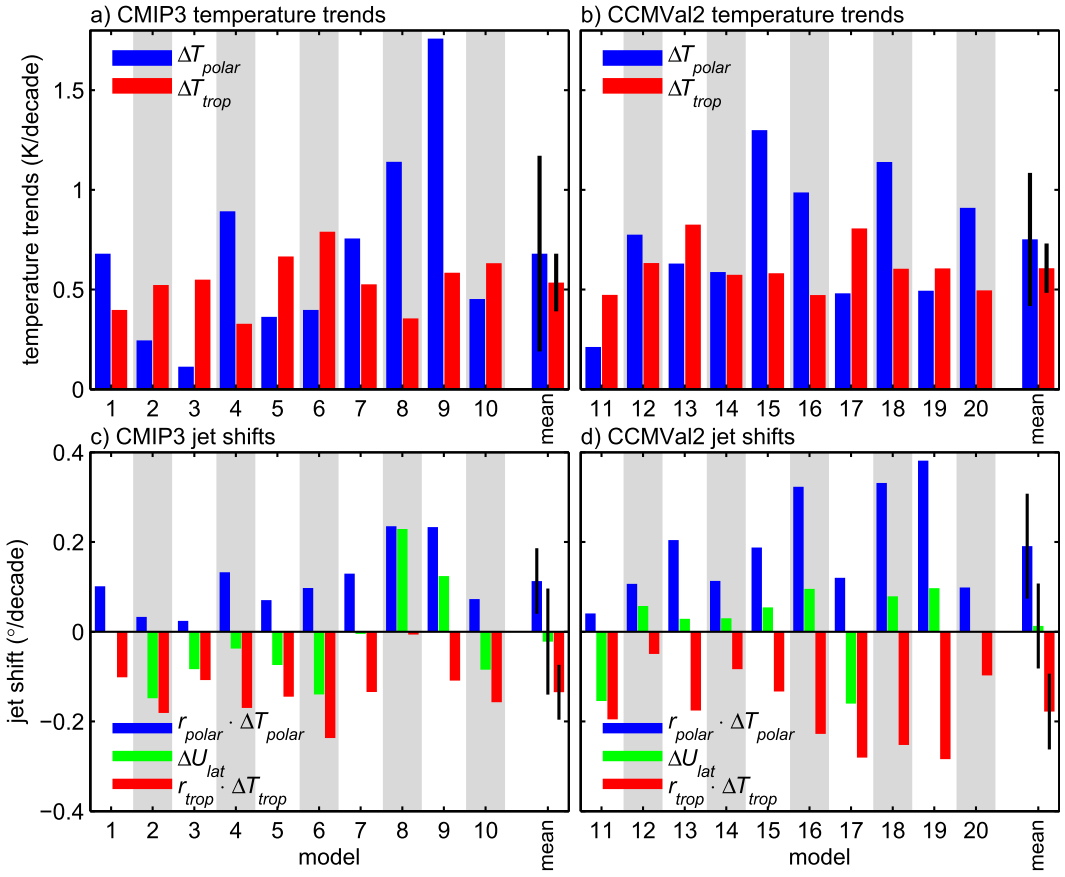

FIG. 5. (a),(b) Temperature and (c),(d) jet shift trends for CMIP3 and CCMVal2 during the period of ozone recovery (2000–79). Here we present the same analysis as in Fig. 4 but for the A1B and REF-B2 scenario integrations of the CMIP3 and CCMVal2 models, respectively. This is an expansion of the multimodel mean analysis shown in Figs. 3d,e.

correlated with tropical temperatures; if this were the only forcing, we would expect the jet to shift poleward. Figure 9c, however, reveals that the difference in polar stratospheric temperatures can explain the opposing jet trends. GFDL CM3, which interactively simulates stratospheric ozone, projects an 11-K warming of the polar stratosphere, in contrast to the modest 2-K warming projected by IPSL-CM5A-MR. Because of these differences in ozone related temperature trends, the gross equator-to-pole temperature difference in the upper troposphere–lower stratosphere decreases in the GFDL model ($4 - 11 = -7$ K) and increases in the IPSL model ($4 - 2 = +2$ K) leading to opposite trends in the jet stream.

The regression coefficients (listed in Figs. 9b,c) allow us to tell a more complete story. In addition to the large difference in polar forcing, IPSL-CMRA-MR is more sensitive to tropical warming, with an r_{trop} value double that found in GFDL CM3: $-0.6°$ versus $-0.3° \text{K}^{-1}$. This suggests the jet would shift farther poleward in the IPSL-CMRA-MR, even if both models had exactly the same trends in polar temperatures.

The importance of differences in the sensitivity of the circulation to temperature changes is highlighted in a second case study in Figs. 9d–f. Here two integrations with divergent trends in the CMIP5 RCP8.5 scenario are shown. The jet barely moves in MIROC-ESM-CHEM (model 41), while it shifts poleward by almost 5° in IPSL-CM5A-MR. This time, however, there is little difference between these models in the temperature trends in the tropics (Fig. 9e) or over the pole (Fig. 9f). Rather, the divergence in jet trends arises from differences in the dynamical response to the temperature trends, which is captured by the regression coefficients in our linear regression analysis. For these two models, it is the sensitivity to tropical temperatures, quantified by r_{trop}, that matters most. The regression analysis suggests that IPSL-CM5A-MR is almost eightfold more sensitive to tropical temperature changes than MIROC-ESM-CHEM.

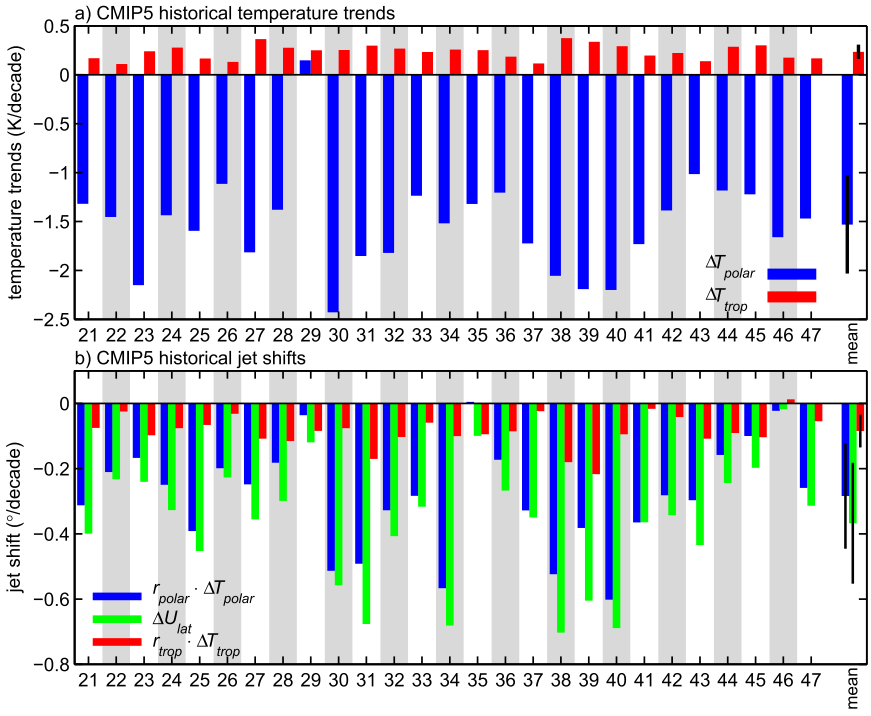

FIG. 6. As in Fig. 4, but for the CMIP5 historical scenario integrations.

Finally, comparison of the IPSL-CM5A-MR trends under the RCP4.5 and RCP8.5 scenarios reveals a third source of spread in jet trends: uncertainty in future CO_2 emissions. The tropical upper troposphere warms almost twice as much under the RCP8.5 scenario (8 K; Fig. 9e) as compared to the RCP4.5 scenario (4 K; Fig. 9b). Based on the regression coefficient for the IPSL-CM5A-MR model ($r_{\text{trop}} = -0.6° \text{K}^{-1}$), this 4-K difference in warming leads to a more poleward trend under the RCP8.5 forcing of approximately 2°.

a. *Uncertainty in the jet shift due to spread in the temperature response to anthropogenic forcing*

The case studies provide anecdotal evidence that differences in temperature trends contribute significantly to intermodel spread. Figure 10 plots the jet trends ΔU_{lat} as a function of ΔT_{trop} and ΔT_{polar} for all of the twenty-first-century model projections. Figure 10a suggests that the degree of tropical warming in a model is a modest predictor of its austral summer jet trend. The shift ΔU_{lat} is −0.45 correlated with ΔT_{trop} across all the integrations, indicating that $R^2 \approx 20\%$ of the variance in jet projections is associated with differences in tropical warming. As shown in Fig. 11, differences in ΔT_{trop} are a comparable predictor of the variance in jet trends in the twentieth-century integrations as well, again associated with about 20% of the spread.

The variance in future tropical temperature trends ΔT_{trop} in Fig. 10a arises from both uncertainty in future greenhouse gas emissions and differences in models' climate sensitivity. The impact of uncertainty in the emissions alone can be assessed by comparing the RCP4.5 and RCP8.5 integrations; these are the exact same models forced with different emissions. As shown in Fig. 3e, under strong forcing in the RCP8.5 scenario, $\Delta U_{\text{lat}} = -0.16° \pm 0.15° \text{ decade}^{-1}$, compared to $-0.05° \pm 0.14° \text{ decade}^{-1}$ in the RCP4.5. The impact of a near doubling of greenhouse emissions on the jet trends is comparable to the standard deviation in trends across models forced by the same emissions.

We can control for uncertainty in the emissions by exploring the spread of models within the individual scenarios, indicated by the different markers in Fig. 10a. We find that the importance of climate sensitivity, manifested as differences in upper-troposphere temperatures, depends on the strength of the greenhouse gas loading. In the CMIP5 RCP4.5 integrations, the correlation between ΔT_{trop} and ΔU_{lat} ($R = 0.18$) is not statistically significant. Thus, differences in upper-tropospheric temperatures are associated with a trivial fraction of the variance, as highlighted in Fig. 12. When the greenhouse emissions are amplified in the RCP8.5 scenario, however, ΔT_{trop} becomes robustly correlated with ΔU_{lat}, and differences in the climate sensitivity are associated with almost 30% of the intermodel spread.

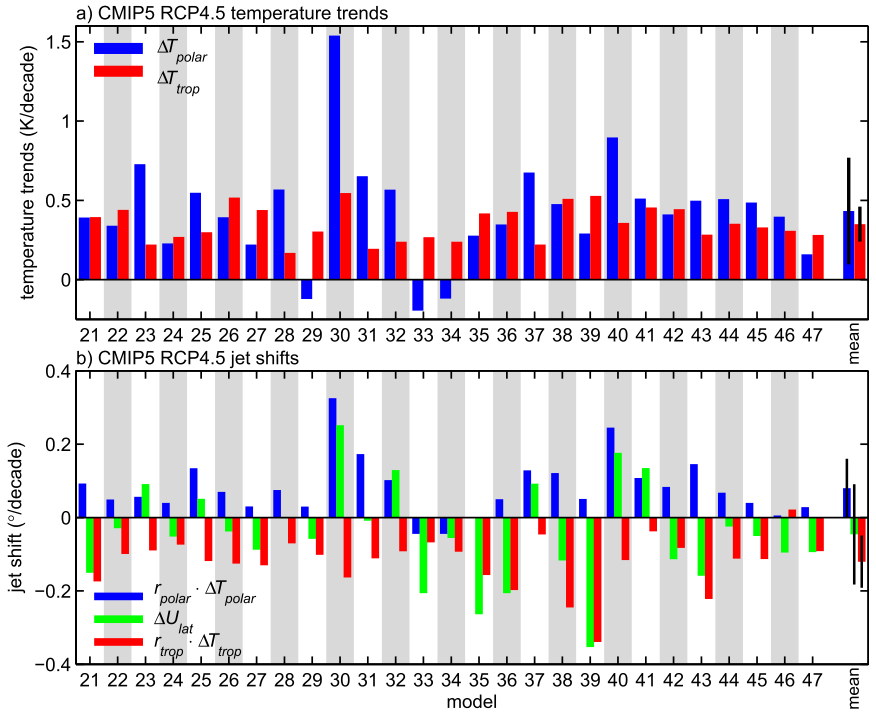

FIG. 7. As in Fig. 5, but for the CMIP5 RCP4.5 scenario integrations. The period of ozone recovery was defined as 2007–79 to avoid interpolation between the historical and future scenarios.

These results support the findings of Arblaster et al. (2011) and Watson et al. (2012), who showed that models with a larger climate sensitivity project a more poleward shift in the austral jet stream in response to greenhouse gas forcing. We add the caveat, however, that this effect can be overwhelmed by other sources of spread, especially with relatively weak emissions, as in the RCP4.5 scenario integrations. Even under the stronger RCP8.5 scenario, it can explain at best 30% of the spread in circulation trends.

We thus turn to differences in polar stratospheric temperatures, shown in Fig. 10b, and find them to be, overall, a stronger predictor of model spread. The correlation between ΔT_{polar} and ΔU_{lat} across all integrations is 0.62, suggesting that nearly 40% of the variance in future projections is associated with differences in temperature trends driven by ozone recovery. Analysis of the late-twentieth-century integrations yields a similar relationship (Fig. 11).

The overall dominance of the polar temperature signal over tropical temperatures can be traced back to the fact that the regression coefficients r_{polar} and r_{trop} are roughly of equivalent amplitude; modifying the gross equator-to-pole temperature difference from either side has a comparable impact on the jet. As seen in Fig. 10, there is simply more spread in polar temperature trends (the standard deviation of ΔT_{polar} 0.34 K decade^{-1} over all twenty-first-century integrations) than in tropical temperature trends, where the standard deviation of ΔT_{trop} is 0.21 K decade^{-1}. The relative importance of polar temperatures diminishes under high CO_2 forcing, however, as shown in Fig. 12. In the RCP8.5 integrations, uncertainty in climate sensitivity leads to greater variance in ΔT_{trop} relative to ΔT_{polar}, and the former becomes the stronger predictor of jet trends.

Spread in ΔT_{polar} may stem from uncertainty in the ozone forcing and/or differences in the thermodynamic response to the ozone changes. Analysis of the CMIP5 models suggests that the former may matter the most, particularly in the future projections. As listed in Table 3, roughly half of the models used the standardized Cionni et al. (2011) ozone dataset or a slight modification thereof to include a solar cycle in the future (Eyring et al. 2013). Based on all the RCP4.5 and RCP8.5 integrations, the standard deviation in ΔT_{polar} is more than double in the models that used their own ozone forcing compared to models with the standard ozone forcing: 0.37 versus 0.15 K decade^{-1}. The mean warming trend associated with ozone recovery, however, is nearly identical in both groups: 0.42 and 0.43 K decade^{-1}, respectively. This suggests that differences in the treatment of ozone inflate the model spread but may not systematically bias the projections.

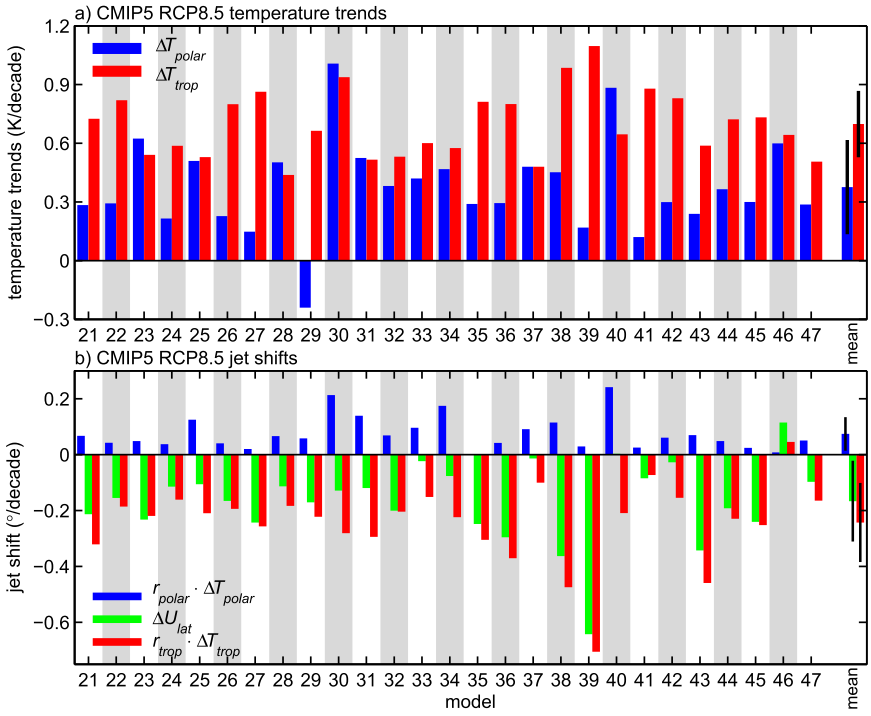

FIG. 8. As in Fig. 7, but for the CMIP5 RCP8.5 scenario integrations.

The standard deviation in ΔT_{polar} in the twenty-first-century CMIP3 and CCMVal2 models is 0.41 K decade^{-1}, comparable to the spread in the CMIP5 models with nonstandard ozone forcing. Polar stratospheric temperature trends were strongly correlated with jet trends in these datasets as well, particularly the CMIP3 models (Fig. 10b). Clearly, a firmer knowledge of the future ozone trends will help reduce the uncertainty in future jet projections.

Taken together, however, differences in both the polar stratospheric and upper-tropospheric temperatures can at best explain half of the spread between models in both the twentieth- and twenty-first-century integrations (Fig. 11). This suggests that reducing the uncertainty in the thermal response to ozone and greenhouse gases may only halve uncertainty in projected summer circulation trends in the Southern Hemisphere.

b. *Uncertainty in the jet shift due to spread in the circulation sensitivity to temperature forcing*

Another source of model spread was highlighted in the second case study in Fig. 9: models with comparable temperature signals (i.e., similar ozone recovery and climate sensitivity) can project very different circulation trends. We describe the circulation response to a given temperature perturbation as a circulation sensitivity, to differentiate it from uncertainty in the temperature trends associated with differences in climate sensitivity and uncertainty in future emissions. The regression coefficients r_{trop} and r_{polar} provide a useful means to quantify the circulation sensitivity of a model.

Overall, models that are more sensitive to tropical temperatures (i.e., with more negative values of r_{trop}) tend to be more sensitive to polar temperatures, exhibiting larger (more positive) values of r_{polar}. The relationship is modest [$\text{corr}(r_{\text{trop}}, r_{\text{polar}}) = -0.32$] but significant at the 95% confidence level. There is greater spread in the values of r_{trop}, with a standard deviation of 0.16° K^{-1} across all models, compared to 0.11° K^{-1} for r_{polar}. The impact of the variance in the circulation sensitivities on the spread in jet shift projections, however, depends on the temperature forcing, as seen in the correlation between the jet stream trends ΔU_{lat} and the regression coefficients r_{trop} and r_{polar} in Fig. 11.

In the historical period, a large fraction of model spread is associated with uncertainty in the sensitivity of the jet to lower-stratospheric cooling over the pole. The -0.61 correlation between r_{polar} and ΔU_{lat} indicates that the jet moves farther poleward in models that are more sensitive to stratospheric temperature trends and that differences in r_{polar} are associated with almost 40% of the total spread in jet trends. Uncertainty in r_{trop}, in comparison, is associated with only about 10% of the spread in jet trends.

In the period of ozone recovery, however, the roles are reversed. Uncertainty in r_{trop}, the circulation sensitivity to

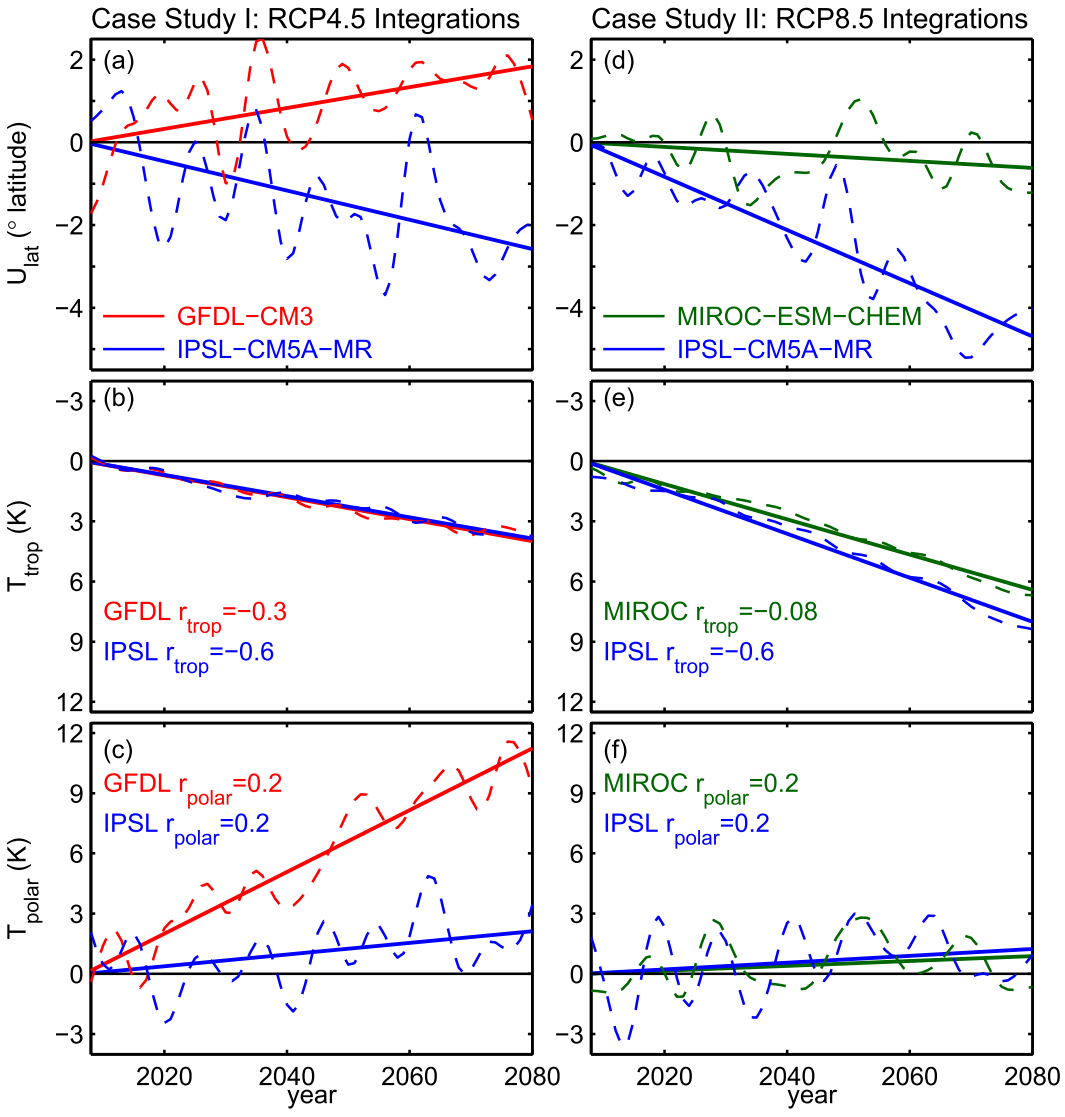

FIG. 9. Two case studies of individual models to illustrate sources of spread in the CMIP5 jet shift projections. (a) Time series of the DJF jet position in RCP4.5 scenario integrations of GFDL CM3 (red) and IPSL-CM5A-MR (blue) models. Here and in the following panels, the dashed curves show the time series relative to 2007 conditions and the solid lines the linear trends. The time series were smoothed by an 8-yr Lanczos filter to remove interannual variability. Changes in (b) DJF tropical (T_{trop}) and (c) ONDJ stratospheric polar cap (T_{polar}) temperatures. The y axis is inverted for the former to visually capture the fact that tropical warming is associated with a negative trend in the jet (i.e., $r_{trop} < 0$). (d)–(f) As in (a)–(c), but for similar analysis of RCP8.5 integrations of the MIROC-ESM-CHEM (green) and IPSL-CM5A-MR (blue) models.

tropical warming, becomes a larger source of model spread and is associated with almost a quarter of the variance in the jet shift projections. In comparison, correlation between r_{polar} and ΔU_{lat} is insignificant in the twenty-first-century integrations and hence associated with trivial fraction of the spread in jet projections.

The flip in importance of r_{polar} and r_{trop} from the past to future periods can be understood in the context of the forcings. The impact of each depends on the temperature trends: that is, jet trends ΔU_{lat} associated with polar cooling are given by $r_{polar}\Delta T_{polar}$. As shown in Fig. 3b, lower-stratospheric cooling associated with ozone loss is almost an order of magnitude larger than warming associated with greenhouse gas warming in the late twentieth century. Hence, uncertainty in the response to polar cooling dominates uncertainty in the response to tropical warming. In the future, however, lower-stratospheric warming associated with ozone

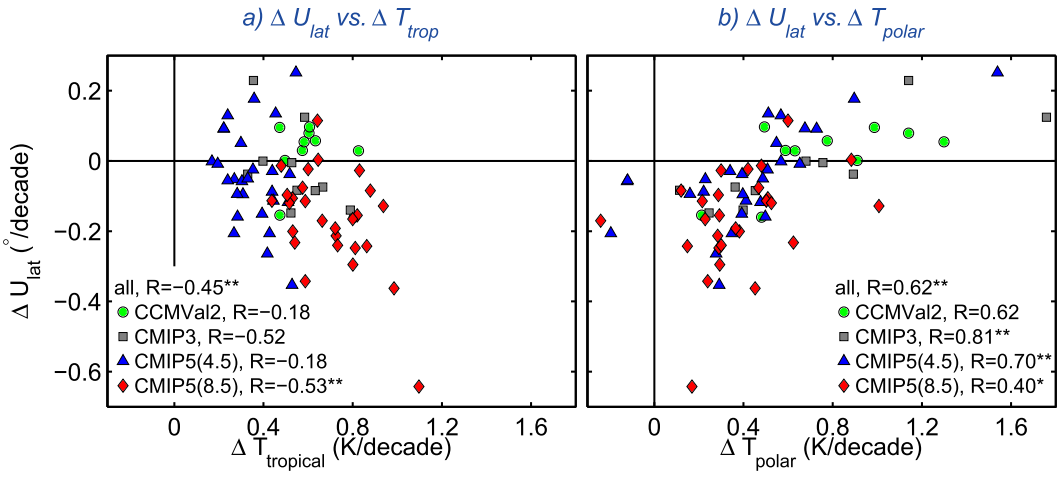

FIG. 10. The relationship between the twenty-first-century shift in the austral jet stream ΔU_{lat} and (a) tropical upper-tropospheric temperatures ΔT_{trop} or (b) polar stratospheric temperatures ΔT_{polar}. Circles, squares, triangles, and diamonds mark CCMVal2 REF-B2, CMIP3 A1B, CMIP5 RCP4.5, and CMIP RCP8.5 model integrations, respectively. The correlation is statistically significant at the 95% or 99% confidence level if marked by one or two asterisks, respectively.

recovery is approximately the same amplitude as warming of the tropics by greenhouse gases. As variability in r_{trop} is larger than r_{polar}, the former plays the dominant role in intermodel differences.

c. *Additional sources of uncertainty in jet trends: Natural variability*

Deser et al. (2012) highlight the fact that circulation trends are inherently less certain than trends in temperatures, emphasizing the greater role of natural variability. We attempted to minimize the impact of variability by first averaging over all available ensemble members for each model, but many modeling groups were only able to submit one integration for archival. As can be seen in time series shown in Fig. 9, natural variability is quite small for tropical temperatures, suggesting that the values for ΔT_{trop} are robust, but could impact polar stratospheric temperatures ΔT_{polar} and the jet trends ΔU_{lat}.

The fact that the standard deviation in ΔT_{polar} doubles in the CMIP5 models that used different ozone forcings suggests that a large fraction of the differences in the temperature trends is indeed forced. This is supported by a comparison of the CMIP3 models with time-varying ozone versus fixed ozone in the appendix, which shows that the spread in ΔT_{polar} increases substantially in the simulations with varying ozone.

Natural variability in ΔU_{lat} that is independent of polar or tropical temperatures would impact the regression coefficients r_{trop} and r_{polar}. For the CMIP5 models, the use of the multiple regression across the historical, RCP4.5, and RCP8.5 scenario integrations was employed to minimize the impact of natural variability. As discussed in section 3, the regression coefficients are more strongly constrained by the historical and RCP8.5 integrations, where the signals (temperature trends ΔT_{polar} and ΔT_{trop}) are stronger.

To quantify the impact of natural variability, we consider the residual δ, defined for each model and scenario integration as

$$\delta = \Delta U_{\text{lat}} - r_{\text{polar}} \Delta T_{\text{polar}} - r_{\text{trop}} \Delta T_{\text{trop}}. \qquad (2)$$

It quantifies the errors in the simple framework for evaluating the jet shifts and may characterize the impact of nonlinearity or natural variability unrelated to temperature trends. The multimodel mean residual is quite small for all scenarios, just 1% of the mean trends associated with polar cooling or tropical warming in the historical and RCP8.5 integrations and 5% of the mean trends in the RCP4.5. That there are little systematic biases in the linear framework suggests that nonlinearity is not a major source of error and that the residuals may largely reflect natural variability.

Figure 12 shows that the residual is highly correlated with ΔU_{lat} in the RCP4.5 integrations. It is associated with roughly 50% of the variance in jet trends and so is slightly more important than ΔT_{polar}. In contrast, the residual is not significantly correlated with ΔU_{lat} in the RCP8.5 integrations. The correlation between jet shifts and the residual is also trivial in the historical integrations ($R = -0.05$). This suggests that natural variability may play a substantial role in the intermodel

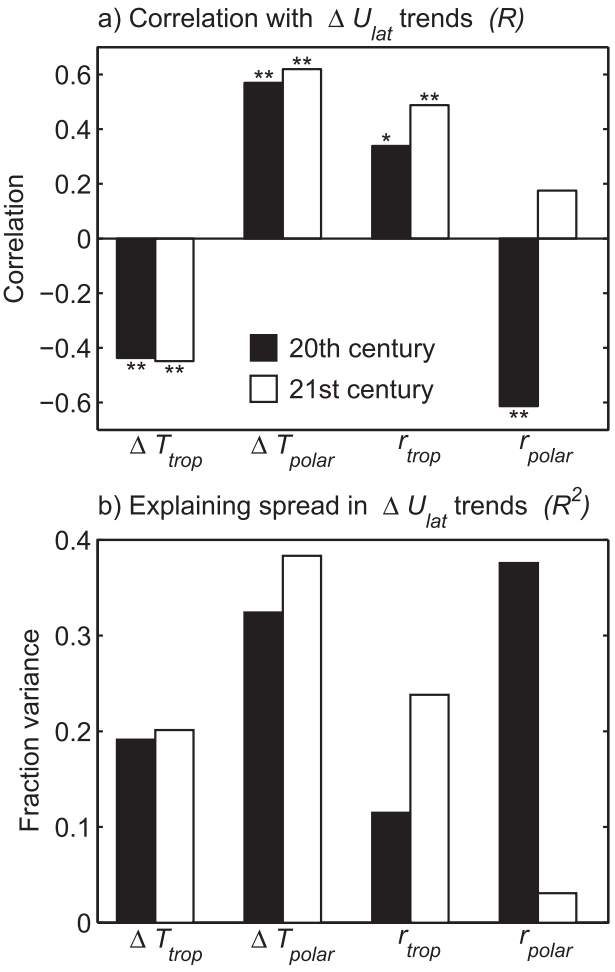

FIG. 11. Identifying the key drivers of the intermodel spread in jet shift trends. (a) The correlation of $\Delta U_{\rm lat}$ trends with $\Delta T_{\rm trop}$, $\Delta T_{\rm polar}$, $r_{\rm trop}$, and $r_{\rm polar}$ across all models for the twentieth-century (black bars) and twenty-first-century (white bars) periods. One or two asterisks mark correlation significant at the 95% or 99% confidence level, respectively. (b) The fraction of the variance in the $\Delta U_{\rm lat}$ trends that can be associated with each parameter over the two time periods. These values are the squares of the correlations shown in (a) and tell us how much of the model spread is associated with variations of a single parameter.

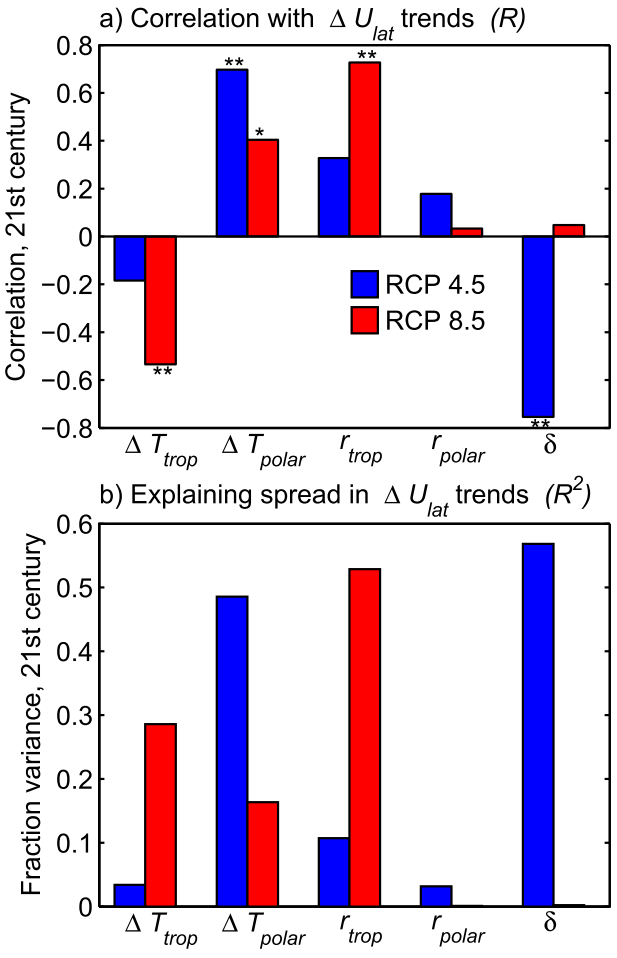

FIG. 12. As in Fig. 11, but focusing on the twenty-first-century CMIP5 RCP4.5 and RCP8.5 scenario integrations, denoted by blue and red bars, respectively. The rightmost bars characterize the spread associated with the residual δ, described in detail in section 5c.

spread in the weakly forced RCP4.5 integrations, while differences in the ozone and greenhouse gas signals dominate the noise in the historical and RCP8.5 scenario integrations. Consistent with the hypothesis, we find that the spread in jet trends is smallest in the RCP4.5 integrations.

6. The Hadley cell

Thus far, we have focused exclusively on the link between tropical and polar temperatures on the eddy driven jet stream. Son et al. (2009) showed that there is a strong linear relationship between shifts in the jet stream and expansion of the Hadley cell in the Southern Hemisphere in summer. Figure 13 is an update of their Fig. 2, where we plot trends in the Hadley cell (defined by the latitude where the 500-hPa streamfunction crosses zero) as a function of trends in the jet stream. During the late twentieth century, the Hadley cell expands poleward during austral summer in nearly all models, while in the twenty-first century trends cluster about zero except for the RCP8.5 integrations, where it continues to expand poleward. There is a strong link between the trend in the jet and the trend in Hadley cell, with an overall correlation of $R = 0.80$, which is highly statistically significant.

As explored in greater detail by Kang and Polvani (2011), there is a 1:2 ratio between shifts in the Hadley cell and jet stream in austral summer: for every 1° that the jet stream shifts poleward, the HC expands

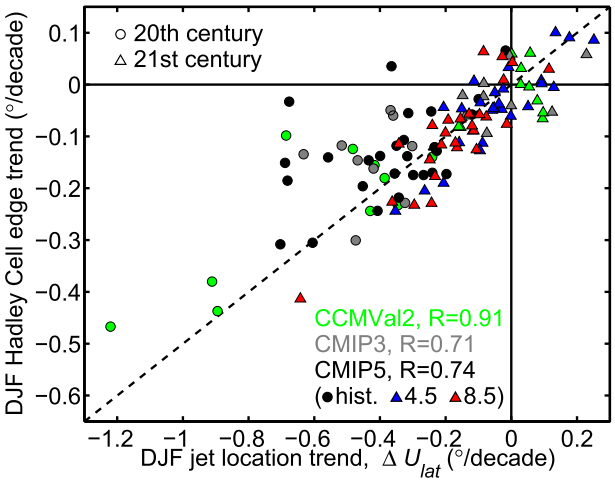

FIG. 13. The relationship between DJF trends in the position of the jet stream (ΔU_{lat}) and the extent of the Hadley cell in the Southern Hemisphere. The dashed line marks the 1:2 trend ratio line, where Hadley cell trends are exactly half that of the jet stream trends. Circles and triangles denote twentieth- and twenty-first-century trends, and colors denote the different datasets. All correlations listed are statistically significant at the 99% confidence level.

approximately ½°. Regression analysis using ΔT_{polar}, ΔT_{trop}, and the Hadley cell trends leads to similar results, except that the regression coefficients are half as large, consistent with this ratio. For the sake of brevity we do not show all these calculations, but emphasize that the key conclusions from our analysis of jet stream trends apply to the Hadley cell as well. In particular, across all twenty-first-century CMIP3, CCMVal2, and CMIP5 integrations, spread in projections of the austral summer Hadley cell expansion is more strongly associated with differences in polar stratospheric temperature trends ΔT_{polar} than tropical temperatures ΔT_{trop}.

7. Summary and discussion

We have assessed changes in the summertime austral circulation over the periods of stratospheric ozone loss and its anticipated recovery in comprehensive climate models from the Chemistry–Climate Model Validation activity 2 (CCMVal2) and phases 3 and 5 of the Coupled Model Intercomparison Project (CMIP3 and CMIP5). Comparison of CMIP3 model integrations with fixed and time-varying ozone suggests that temperature trends in the lower polar stratosphere and upper tropical troposphere can be linked to changes in ozone and greenhouse gases, respectively. We developed a simple framework to connect shifts in the jet stream to these temperature trends, which allows us to partition the influence of stratospheric ozone and greenhouses gases on circulation trends and investigate sources of intermodel spread in the projections.

We find that the latitudes of the jet and Hadley cell boundary are sensitive to the temperature gradient between the tropics and high latitudes in the upper troposphere–lower stratosphere, supporting the findings of Arblaster et al. (2011) and Wilcox et al. (2012). The circulation shifts poleward when the gradient is increased and appears comparably sensitive to temperature perturbations on either side. On average, a 1-K increase of the equator-to-pole temperature difference by greenhouse gas–induced warming of the tropical upper troposphere drives the jet stream 0.3° poleward. A 1-K decrease in the temperature difference associated with a warming of the polar lower stratosphere (as expected with ozone recovery) shifts it 0.2° equatorward. The Hadley cell responds similarly but with half the amplitude.

The mean response of the circulation is fairly consistent across each multimodel dataset, as summarized in Fig. 3. From 1960 to 1999, models shift the austral jet poleward approximately 1°–2°. The bulk of the trend is driven by cooling of the polar stratosphere associated with ozone loss. Over the period of ozone recovery (2000–79 or 2007–79), models project little change in the jet stream, because of cancellation between the effects of greenhouse gas emissions and stratospheric ozone recovery on the equator-to-pole temperature gradient. Under stronger greenhouse gas forcing in the CMIP5 RCP8.5 scenario, however, global warming tends to dominate ozone recovery and the jet shifts poleward, albeit more slowly than in the late twentieth century. These findings support the conclusions of previous studies based on individual models (Gillett and Thompson 2003; Arblaster and Meehl 2006; Perlwitz et al. 2008; Polvani et al. 2011; McLandress et al. 2011); multimodel datasets (Son et al. 2008, 2010; Barnes et al. 2014); and, for the historic period, observations (Lee and Feldstein 2013).

Over the period of ozone loss, the CCMVal2 models exhibit a stronger poleward shift of the jet. In comparison to the CMIP3 models, this difference cannot be attributed to differences in the temperature trends. Rather, these CCMVal2 models are more sensitive to polar cooling (i.e., exhibit larger coefficients r_{polar}), possibly because they capture the nonzonal structure of ozone loss, which has been shown to increase the sensitivity of the tropospheric jet (e.g., Crook et al. 2008; Waugh et al. 2009). The response is slightly weaker in the CMIP5 models and can be attributed to weaker cooling in the polar stratosphere and reduced sensitivity.

The consistency of the multimodel mean datasets may give a false sense of certainty; we cannot detect statistically significant differences between CCMVal2 and CMIP models largely because the intermodel spread is

so great. Even over the past period, where the forcings are better constrained, models simulate a wide range of jet shifts: in one model the jet stream is essentially fixed, while in another it shifts nearly 5° poleward. In the future, the spread in model jet shift projections expands to almost 7°, with one model moving the jet 2° equatorward and another shifting it 5° poleward.

Our simple framework suggests that roughly half of these intermodel differences are associated with uncertainty in the temperature response of the upper troposphere–lower stratosphere to anthropogenic forcing. Differences in the ozone driven temperature signal in the lower polar stratospheric are associated with approximately 35% of the total variance in future jet stream trends over the period of ozone recovery. In comparison, differences in greenhouse gas driven warming of the tropical upper troposphere are associated with roughly 20% of the spread in jet trends. Uncertainty in future temperature trends arises from both uncertainty in future atmospheric composition changes (emissions uncertainty and ozone chemistry) and the atmospheric response to these changes in composition (i.e., climate sensitivity).

The multimodel mean difference in jet trends between the CMIP5 RCP4.5 and RCP8.5 scenarios is comparable to the spread in jet trends within a given scenario, suggesting that both uncertainty in emissions and climate sensitivity matter. Our results support the conclusions of Arblaster et al. (2011) and Watson et al. (2012) that the jet shifts more poleward in models with greater climate sensitivity, but with the caveat that this effect may be overwhelmed by other differences until the greenhouse gas loading becomes sufficiently strong. In the RCP8.5 integrations, differences in tropical upper-troposphere warming (which is highly correlated with climate sensitivity) are associated with 30% of the spread in jet projections, while, in the RCP4.5, differences in warming have a trivial impact.

Overall, differences in the cooling or warming associated with ozone loss or recovery appear to be more influential than differences in tropical warming because of greater spread in lower polar stratospheric temperature trends. Much of the difference in the polar stratospheric temperature trends may be attributed to differences in ozone. The variance in polar stratospheric temperature trends is 6 times greater in models that use individualized ozone forcing (models with interactive chemistry or custom prescribed ozone) compared to the CMIP5 models using the standardized Cionni et al. (2011) ozone dataset.

In principle, observations of stratospheric ozone should constrain both past and future trends (in that the amplitude of ozone recovery is related to the initial loss), allowing one to reduce the uncertainty in polar stratospheric temperature trends. There are significant differences in observationally based datasets, however, related largely to choices in the regression model (Hassler et al. 2013). This leads to differences in the estimate of ozone loss that can alter the total radiative forcing by a factor of 4 and suggests that further observations of stratospheric ozone could reduce uncertainty in future circulation trends.

The other half of intermodel spread in the circulation trends is independent of upper-troposphere–lower-stratosphere temperature gradients. To differentiate this uncertainty from radiative forcing, we call it a circulation sensitivity. Even if the climate sensitivity and the response of the stratosphere to ozone were known with absolute certainty, there would still be considerable spread in the circulation response. The circulation sensitivity can be quantified by the regression coefficients r_{trop} and r_{polar}. We find that there is greater intermodel spread in r_{trop}. Thus, while there is greater uncertainty in polar trends $\Delta T_{\mathrm{polar}}$ compared to ΔT_{trop}, overall the total spread in jet projections associated with ozone and greenhouse gases is comparable.

The spread in the circulation sensitivity may stem in part from differences in the spatial structure of warming, which are not accounted for in our simple framework. In particular, Tandon et al. (2013) suggest that warming in the subtropics may play a stronger role in jet trends. Uncertainty may also stem from problems in our ability to simulate large-scale dynamics. Kidston and Gerber (2010) and Barnes and Hartmann (2010) show that biases in the climatology and large-scale variability in climate models may be linked to their sensitivity to external forcing. Twenty-first-century jet shifts tend to be stronger in models with an equatorward bias of the jet stream in their historical simulations, and biases in the climatology are associated with enhanced persistence in the southern annular mode, reflecting stronger eddy–mean flow feedback. These biases were pretty extreme in some CCMVal2 models (Son et al. 2010) and could explain their heightened sensitivity.

It is also important to acknowledge that our simple framework based on upper-troposphere–lower-stratosphere temperatures may not properly account for the impacts of other processes that do not directly modify this temperature gradient. Changes in aerosols (Gillett et al. 2013), tropical convection (Ceppi et al. 2013), and clouds (Trenberth and Fasullo 2010) can impact jet trends, and uncertainties in these processes may lead to greater spread in the regression coefficients. Natural variability also contributes significantly to uncertainty in circulation trends, particularly in the more weakly forced RCP4.5 scenario integrations, where half of the variance in jet trends could not be captured by the regression model.

Our analysis of the jet stream response in comprehensive models has implications for understanding the

mechanism(s) by which greenhouse gases and ozone changes affect the circulation. As reviewed in Gerber et al. (2012) and Garfinkel et al. (2013), a number of mechanisms have been proposed to explain how a cooling of the stratosphere induces a change in the tropospheric jet stream. Most studies have viewed the response to tropical warming separately from the response to polar stratospheric cooling, with the former suggesting a baroclinic mechanism (e.g., Butler et al. 2011) and the latter suggesting a barotropic mechanism (e.g., Simpson et al. 2009). Our finding that the $r_{\text{polar}} \sim -r_{\text{trop}}$ indicates that the jet response is qualitatively the same whether the upper-troposphere–lower-stratosphere temperature gradient is changed from the tropics or the high latitudes. This hints that a common mechanism may explain the response of the jet stream to both greenhouse gas and stratospheric ozone changes. Riviére (2011) focuses on the impact of upper-tropospheric temperature gradients on baroclinic instability and the resulting eddy momentum fluxes, providing a promising step in this direction.

Acknowledgments. We thank Alexey Karpechko, Lorenzo Polvani, Peter Watson, Laura Wilcox, and an anonymous reviewer for constructive comments on an earlier manuscript and Jung Choi for computing the Hadley cell trends of the CMIP5 scenario integrations. We acknowledge the World Climate Research Programme's (WCRP) Working Group on Coupled Modelling, which is responsible for coordinating the CMIP3 and CMIP5 activities, and WCRP's SPARC project, which coordinated the CCMVal2 activity, and thank the climate modeling groups for producing and making available their model output. For the CMIP, the U.S. Department of Energy's Program for Climate Model Diagnosis and Intercomparison provided coordinating support and led development of software infrastructure in partnership with the Global Organization for Earth System Science Portals. For the CCMVal2, model output was collected and archived by the British Atmospheric Data Center. EPG acknowledges support from the U.S. National Science Foundation under Grant AGS-1264195 and SWS support from the Basic Science Research Program through the National Research Foundation of Korea (NRF) funded by the Ministry of Education (2013R1A1A1006530).

APPENDIX

Is Global Warming Aliasing onto Stratospheric Polar Temperature Trends?

While greenhouse gases warm the troposphere, they cool the stratosphere, particularly at upper levels. We were therefore concerned that the stratospheric trends ΔT_{polar} might be driven in part by greenhouse gas changes. A resulting negative correlation between ΔT_{polar} and ΔT_{trop} could cause our method to overestimate the shift in the jet stream associated with stratospheric cooling in the late twentieth century and potentially underestimate the impact of warming during the recovery in this century. The eight CMIP3 integrations with fixed ozone in both the historic and future periods allow us to explore whether this aliasing is cause for concern. In these simulations, stratospheric trends are associated only with global warming or natural variability. Our analysis, summarized in Fig. A1, suggests that the effect of aliasing is small.

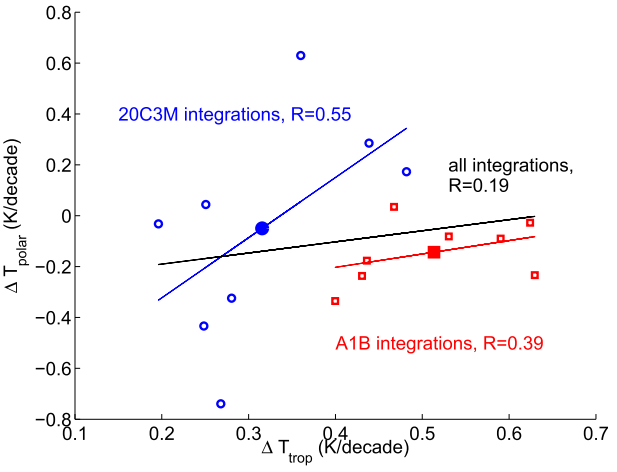

FIG. A1. The relationship between tropical upper-tropospheric warming ΔT_{trop} and polar stratospheric cooling ΔT_{polar} in integrations of CMIP3 models with fixed ozone.

Considering both the 20C3M and A1B scenario integrations together, ΔT_{polar} and ΔT_{trop} are not significantly correlated ($R = 0.19$). The sign of the correlation, however, is opposite to what we initially expected: integrations with larger warming in the tropics generally exhibit weaker cooling (or even warming) over the austral polar cap. The positive correlation suggests that our framework could actually overestimate the impact of tropical warming, in that models that warm the troposphere more strongly will exhibit less cooling or more warming the stratosphere, but we should not overinterpret this statistically insignificant relationship. Most important for our purposes is that the regression coefficient between the tropical warming and polar cooling is small. Thus, any action to remove the signal of greenhouse gases in the polar stratosphere by regression would have little effect.

When we look at the scenario integrations separately, we obtain similar findings. The temperatures are slightly

more correlated, particularly in the historic 20C3M integrations, but the correlation is positive and statistically insignificant. It is only when we compare the multimodel means for the past and future trends that we see the negative correlation between tropical warming and stratospheric cooling that we expected.

The spread in stratospheric cooling trends, particularly in the historic simulations, does suggest that natural variability will be more pronounced over the polar cap. Natural variability leads to a spread of 0.4 and 0.1 in the twentieth- and twenty-first-century simulations, respectively. Greater uncertainty in the earlier period is consistent with the shorter time period. This is substantially smaller than the spread in the simulations with time-varying ozone (0.8 and 0.4 for the two periods, respectively, as shown in Fig. 3), suggesting that the differences in the forced integrations are primarily driven by differences in ozone forcing, particularly in the twenty-first-century period of ozone recovery.

It was suggested by Hu et al. (2011) that ozone recovery may impact tropospheric temperatures, raising the possibility that ozone trends could alias onto ΔT_{trop}. We found little difference in tropospheric temperature trends in the CMIP3 models with fixed versus time-varying ozone, as shown in Fig. 1, suggesting that the effect is fairly minor. In a more controlled study, McLandress et al. (2012) found that ozone had little impact on tropical tropospheric temperatures and that the differences observed by Hu et al. (2011) may rather reflect differences in climate sensitivity.

REFERENCES

Arblaster, J. M., and G. A. Meehl, 2006: Contributions of external forcings to southern annular mode trends. *J. Climate,* **19,** 2896–2905, doi:10.1175/JCLI3774.1.

——, ——, and D. J. Karoly, 2011: Future climate change in the Southern Hemisphere: Competing effects of ozone and greenhouse gases. *Geophys. Res. Lett.,* **38,** L02701, doi:10.1029/2010GL045384.

Barnes, E. A., and D. L. Hartmann, 2010: Testing a theory for the effect of latitude on the persistence of eddy-driven jets using CMIP3 simulations. *Geophys. Res. Lett.,* **37,** L15801, doi:10.1029/2010GL044144.

——, N. W. Barnes, and L. M. Polvani, 2014: Delayed Southern Hemisphere climate change induced by stratospheric ozone recovery, as projected by the CMIP5 models. *J. Climate,* **27,** 852–867, doi:10.1175/JCLI-D-13-00246.1.

Butler, A. H., D. W. J. Thompson, and R. Heikes, 2010: The steady-state atmospheric circulation response to climate change–like thermal forcings in a simple general circulation model. *J. Climate,* **23,** 3474–3496, doi:10.1175/2010JCLI3228.1.

——, ——, and T. Birner, 2011: Isentropic slopes, downgradient eddy fluxes, and the extratropical atmospheric circulation response to tropical tropospheric heating. *J. Atmos. Sci.,* **68,** 2292–2305, doi:10.1175/JAS-D-10-05025.1.

Ceppi, P., Y.-T. Hwang, X. Liu, D. M. W. Frierson, and D. L. Hartmann, 2013: The relationship between the ITCZ and the Southern Hemisphere eddy-driven jet. *J. Geophys. Res. Atmos.,* **118,** 5136–5146, doi:10.1002/jgrd.50461.

Charlton-Perez, A. J., and Coauthors, 2013: On the lack of stratospheric dynamical variability in low-top versions of the CMIP5 models. *J. Geophys. Res. Atmos.,* **118,** 2494–2505, doi:10.1002/jgrd.50125.

Cionni, I., and Coauthors, 2011: Ozone database in support of CMIP5 simulations: Results and corresponding radiative forcing. *Atmos. Chem. Phys.,* **11,** 11 267–11 292, doi:10.5194/acp-11-11267-2011.

Crook, J. A., N. P. Gillett, and S. P. E. Keeley, 2008: Sensitivity of Southern Hemisphere climate to zonal asymmetry in ozone. *Geophys. Res. Lett.,* **35,** L07806, doi:10.1029/2007GL032698.

Deser, C., A. Phillips, V. Bourdette, and H. Teng, 2012: Uncertainty in climate change projections: The role of internal variability. *Climate Dyn.,* **38,** 527–546, doi:10.1007/s00382-010-0977-x.

Eyring, V., T. G. Shepherd, and D. W. Waugh, Eds., 2010: Chemistry-climate model validation. SPARC Rep. 5, 426 pp. [Available online at http://www.sparc-climate.org/publications/sparc-reports/sparc-report-no5/.]

——, and Coauthors, 2013: Long-term ozone changes and associated climate impacts in CMIP5 simulations. *J. Geophys. Res. Atmos.,* **118,** 5029–5060, doi:10.1002/jgrd.50316.

Farman, J. C., B. G. Gardiner, and J. D. Shanklin, 1985: Large losses in total ozone in Antarctica reveal seasonal ClO_x/NO_x interaction. *Nature,* **315,** 207–210, doi:10.1038/315207a0.

Garfinkel, C. I., D. W. Waugh, and E. P. Gerber, 2013: The effect of tropospheric jet latitude on coupling between the stratospheric polar vortex and the troposphere. *J. Climate,* **26,** 2077–2095, doi:10.1175/JCLI-D-12-00301.1.

Gerber, E. P., and Coauthors, 2012: Assessing and understanding the impact of stratospheric dynamics and variability on the Earth system. *Bull. Amer. Meteor. Soc.,* **93,** 845–859, doi:10.1175/BAMS-D-11-00145.1.

Gillett, N. P., and D. W. J. Thompson, 2003: Simulation of recent Southern Hemisphere climate change. *Science,* **302,** 273–275, doi:10.1126/science.1087440.

——, J. C. Fyfe, and D. E. Parker, 2013: Attribution of observed sea level pressure trends to greenhouse gas, aerosol and ozone changes. *Geophys. Res. Lett.,* **40,** 2302–2306, doi:10.1002/grl.50500.

Hassler, B., P. J. Young, R. W. Portmann, G. E. Bodeker, J. S. Daniel, K. H. Rosenlof, and S. Solomon, 2013: Comparison of three vertically resolved ozone data sets: Climatology, trends and radiative forcings. *Atmos. Chem. Phys.,* **13,** 5533–5550, doi:10.5194/acp-13-5533-2013.

Hu, Y., Y. Xia, and Q. Fu, 2011: Tropospheric temperature response to stratospheric ozone recovery in the 21st century. *Atmos. Chem. Phys.,* **11,** 7687–7699, doi:10.5194/acp-11-7687-2011.

Kang, S., and L. M. Polvani, 2011: The interannual relationship between the latitude of the eddy-driven jet and the edge of the Hadley cell. *J. Climate,* **24,** 563–568, doi:10.1175/2010JCLI4077.1.

——, ——, J. C. Fyfe, and M. Sigmond, 2011: Impact of polar ozone depletion on subtropical precipitation. *Science,* **332,** 951–954, doi:10.1126/science.1202131.

Kidston, J., and E. P. Gerber, 2010: Intermodel variability of the poleward shift of the austral jet stream in the CMIP3 integrations linked to biases in 20th century climatology. *Geophys. Res. Lett.,* **37,** L09708, doi:10.1029/2010GL042873.

Kushner, P. J., I. M. Held, and T. L. Delworth, 2001: Southern Hemisphere atmospheric circulation response to global warming. *J. Climate,* **14,** 2238–2249, doi:10.1175/1520-0442(2001)014<0001:SHACRT>2.0.CO;2.

Lee, S., and S. B. Feldstein, 2013: Detecting ozone- and greenhouse gas–driven wind trends with observational data. *Science,* **339,** 563–567, doi:10.1126/science.1225154.

Lorenz, E. N., 1967: *The Nature and Theory of the General Circulation of the Atmosphere*. World Meteorological Organization, 161 pp.

Marshall, G. J., 2003: Trends in the southern annular mode from observations and reanalyses. *J. Climate,* **16,** 4134–4143, doi:10.1175/1520-0442(2003)016<4134:TITSAM>2.0.CO;2.

McLandress, C., T. G. Shepherd, J. F. Scinocca, D. A. Plummer, M. Sigmond, A. I. Jonsson, and M. C. Reader, 2011: Separating the dynamical effects of climate change and ozone depletion. Part II: Southern Hemisphere troposphere. *J. Climate,* **24,** 1850–1868, doi:10.1175/2010JCLI3958.1.

——, J. Perlwitz, and T. G. Shepherd, 2012: Comment on ''Tropospheric temperature response to stratospheric ozone recovery in the 21st century'' by Hu et al. (2011). *Atmos. Chem. Phys.,* **12,** 2533–2540, doi:10.5194/acp-12-2533-2012.

Meehl, G. A., C. Covey, T. Delworth, M. Latif, B. McAvaney, J. F. B. Mitchell, R. J. Stouffer, and K. E. Taylor, 2007: The WCRP CMIP3 multimodel dataset. *Bull. Amer. Meteor. Soc.,* **88,** 1383–1394, doi:10.1175/BAMS-88-9-1383.

Perlwitz, J., S. Pawson, R. L. Fogt, J. E. Nielsen, and W. D. Neff, 2008: The impact of stratospheric ozone hole recovery on Antarctic climate. *Geophys. Res. Lett.,* **35,** L08714, doi:10.1029/2008GL033317.

Polvani, L. M., and P. J. Kushner, 2002: Tropospheric response to stratospheric perturbations in a relatively simple general circulation model. *Geophys. Res. Lett.,* **29**, doi:10.1029/2001GL014284.

——, D. W. Waugh, G. J. P. Correa, and S.-W. Son, 2011: Stratospheric ozone depletion: The main driver of twentieth-century atmospheric circulation changes in the Southern Hemisphere. *J. Climate,* **24,** 795–812, doi:10.1175/2010JCLI3772.1.

Riviére, G., 2011: A dynamical interpretation of the poleward shift of the jet streams in global warming scenarios. *J. Atmos. Sci.,* **68,** 1253–1272, doi:10.1175/2011JAS3641.1.

Seidel, D. J., and W. J. Randel, 2007: Recent widening of the tropical belt: Evidence from tropopause observations. *J. Geophys. Res.,* **112,** D20113, doi:10.1029/2007JD008861.

Simpson, I. R., M. Blackburn, and J. D. Haigh, 2009: The role of eddies in driving the tropospheric response to stratospheric heating perturbations. *J. Atmos. Sci.,* **66,** 1347–1365, doi:10.1175/2008JAS2758.1.

Son, S.-W., and Coauthors, 2008: The impact of stratospheric ozone recovery on the Southern Hemisphere westerly jet. *Science,* **320,** 1486–1489, doi:10.1126/science.1155939.

——, N. F. Tandon, L. M. Polvani, and D. W. Waugh, 2009: Ozone hole and Southern Hemisphere climate change. *Geophys. Res. Lett.,* **36,** L15705, doi:10.1029/2009GL038671.

——, and Coauthors, 2010: The impact of stratospheric ozone on Southern Hemisphere circulation change: A multimodel assessment. *J. Geophys. Res.,* **115,** D00M07, doi:10.1029/2010JD014271.

Tandon, N. F., E. P. Gerber, A. H. Sobel, and L. M. Polvani, 2013: Contrasting the circulation response to El Niño and global warming. *J. Climate,* **26,** 4304–4321, doi:10.1175/JCLI-D-12-00598.1.

Taylor, K. E., R. J. Stouffer, and G. A. Meehl, 2012: An overview of CMIP5 and the experiment design. *Bull. Amer. Meteor. Soc.,* **93,** 485–498, doi:10.1175/BAMS-D-11-00094.1.

Thompson, D. W. J., and S. Solomon, 2002: Interpretation of recent Southern Hemisphere climate change. *Science,* **296,** 895–899, doi:10.1126/science.1069270.

——, ——, P. J. Kushner, M. H. England, K. M. Grise, and D. J. Karoly, 2011: Signatures of the Antarctic ozone hole in Southern Hemisphere surface climate change. *Nat. Geosci.,* **4,** 741–749, doi:10.1038/ngeo1296.

Trenberth, K. E., and J. T. Fasullo, 2010: Simulation of present-day and twenty-first-century energy budgets of the Southern Oceans. *J. Climate,* **23,** 440–454, doi:10.1175/2009JCLI3152.1.

Wang, S., E. P. Gerber, and L. M. Polvani, 2012: Abrupt circulation responses to upper-tropospheric warming in a relatively simple stratosphere-resolving AGCM. *J. Climate,* **25,** 5097–4115, doi:10.1175/JCLI-D-11-00166.1.

Watson, P. A. G., D. J. Karoly, M. R. Allen, N. Faull, and D. S. Lee, 2012: Quantifying uncertainty in future Southern Hemisphere circulation trends. *Geophys. Res. Lett.,* **39,** L23708, doi:10.1029/2012GL054158.

Waugh, D. W., L. Oman, P. A. Newman, R. S. Stolarski, S. Pawson, J. E. Nielsen, and J. Perlwitz, 2009: Effect of zonal asymmetries in stratospheric ozone on simulated Southern Hemisphere climate trends. *Geophys. Res. Lett.,* **36,** L18701, doi:10.1029/2009GL040419.

——, F. Primeau, T. DeVries, and M. Holzer, 2013: Recent changes in ventilation of the southern oceans. *Science,* **339,** 568–570, doi:10.1126/science.1225411.

Wilcox, L. J., A. J. Charlton-Perez, and L. J. Gray, 2012: Trends in austral jet position in ensembles of high- and low-top CMIP5 models. *J. Geophys. Res.,* **117,** D13115, doi:10.1029/2012JD017597.

Yin, J. H., 2005: A consistent poleward shift of the storm tracks in simulations of 21st century climate. *Geophys. Res. Lett.,* **32,** L18701, doi:10.1029/2005GL023684.